New Peak-to-Average Power Ratio Reduction Schemes for OFDM Systems

Peng Liu

A Thesis

in

The Department

of

Electrical and Computer Engineering

Presented in Partial Fulfillment of the Requirements

for the Degree of Master of Applied Science at

Concordia University

Montreal, Quebec, Canada

January 2004

Your file Votre référence
ISBN: 0-612-91071-7
Our file Notre référence
ISBN: 0-612-91071-7

ABSTRACT

New Peak-to-Average Power Ratio Reduction Schemes for OFDM Systems

Peng Liu

It is known that the orthogonal frequency division multiplexing (OFDM) modulation is very suitable for high-speed wireless transmission systems due to its bandwidth efficiency and ability in coping with multipath fading. However, the large peak-to-average power ratio (PAPR) of an OFDM signal limits the application of OFDM to a certain degree.

The research focus of this thesis is on the study of some new PAPR reduction schemes for OFDM systems. In the first part of the thesis, we investigate the peak windowing method, the clipping method, and a combination of the two techniques with an emphasis on the performance assessment of the transmitted OFDM signal using the combination scheme. We start with the review of the two typical signal distortion techniques and point out their advantages and shortcomings. We then propose a combination scheme for the two techniques in order to overcome their drawbacks. In the proposed combination scheme, a weighting function is used to remove instantaneous signal peaks and then a hard-limiting is utilized for the reduction of the overall peak powers. A modified IDFT interpolation is developed and employed in the combination scheme to improve the

interpolation precision of the time-domain OFDM signal. The performance of the proposed combination scheme, that is, the bit error rate (BER) and the out-of-band radiation of the OFDM signal spectrum, is analyzed through computer simulation and is also compared with that of the existing distortion methods.

The second part of the thesis is concerned with a class of non-signal-distorted PAPR reduction techniques using the so-called partial transmit sequences (PTS). A phase adjustment PTS (PAPTS) method is first proposed, which seeks a set of optimum phase factors for the combination of signal subblocks in order to minimize the PAPR. The second PAPR reduction scheme proposed in this aspect is the amplitude adjustment based PTS (AAPTS) method. This method is to determine a set of amplitude factors or gains for signal subblocks in order to find a combination of these subblocks that achieves the minimum PAPR. The proposed PAPTS and AAPTS techniques can reduce the computational complexity of the conventional PTS method and increase the system flexibility as a result of making full use of the continuous phase/amplitude adjustment in the search process. The performances of the new schemes are evaluated through extensive simulations carried out using the Matlab software package for various parameters such as the number of signal subblocks, the number of iterations and the signal-to-noise ratio. It is demonstrated that the proposed schemes provide significant computational savings while yielding a PAPR reduction performance that is similar to that of the conventional PTS method.

Dedicated to my cute son.

ACKNOWLEDGEMENTS

First, I would like to express my sincere gratitude to my supervisors, Dr. M.O. Ahmad, and Dr. W.-P. Zhu for their invaluable guidance, encouragement, and support that made this work possible. I am grateful for their extremely careful and thorough review of my thesis, and for their inspiration throughout the course of this work. I feel privileged for having the opportunity to work under their supervision and I am looking forward to maintaining a continued friendship with them. I would also like to thank all my teachers who were of great support throughout my academic life.

I am also grateful to all my friends and colleagues for their help and advice.

Most of all, I would like to thank my wife for her love and understanding. I could not have completed my degree without her continuous and immeasurable support.

Finally, I am heartily grateful to my parents for their endless love, support and encouragement throughout my life.

TABLE OF CONTENTS

LIST OF TABLES

LIST OF FIGURES

LIST OF ABBREVIATIONS AND SYMBOLS

AAPTS	Amplitude Adjustment Partial Transmit Sequence
ADSL	Asymmetric Digital Subscriber Lines
AWGN	Additive White Gaussian Noise
A/D	Analog-to-Digital
BER	Bit Error Rate
BPSK	Binary Phase-Shift Keying
CCDF	Complementary Cumulative Distributed Function
CDF	Cumulative Distribution Function
CDMA	Code-Division Multiple Access
CR	Clipping Ratio
DAB	Digital Audio Broadcasting
DFT	Discrete Fourier Transform
DVB	Digital Video Broadcasting
D/A	Digital-to-Analog
FDM	Frequency Division Multiplexing
FFT	Fast Fourier Transform
HDTV	High-Definition Television
HIPERLAN	High Performance Local Area Network
ICI	Inter Carrier Interference
IDFT	Inverse Discrete Fourier Transform
IFFT	Inverse Fast Fourier Transform
ISI	Intersymbol Interference

LPF	Low-Pass Filtering
MCM	Multicarrier Modulation
OFDM	Orthogonal Frequency Division Multiplexing
PAPR	Peak-to-Average Power Ratio
PAPTS	Phase Adjustment Partial Transmit Sequence
PC	Peak Cancellation
PDF	Probability Density Function
PSD	Power Spectral Density
PSK	Phase-Shift Keying
PTS	Partial Transmit Sequence
P/S	Parallel-to-Series
QAM	Quadrature Amplitude Modulation
QPSK	Quadrature Phase-Shift Keying
RF	Radio Frequency
SLM	Selected Mapping
SNR	Signal-to-Noise Ratio
S/P	Series-to-Parallel
WLAN	Wireless Local Area Networks

R	Bit rate of original data stream.
d_i	The i^{th} transmitted symbol.
N	Number of subcarriers.
T	Symbol duration.
t_s	Starting time of the OFDM symbol.
a_n	Transmitted information symbol in the n^{th} subchannel
σ_a	Standard deviation.
α	Weighting coefficient.
$\mathbf{A}$	Input data vector for the IDFT block.
$\mathbf{a}$	IDFT of **A**.
s	Original time-domain OFDM signal.
S	Original frequency-domain OFDM signal.
v	Interpolated time-domain OFDM signal.
V	Interpolated frequency-domain OFDM signal.
$\hat{e}$	Total interpolation error.
p	Probability density function
s_E	Envelop of the OFDM signal.
w	Window function.
t'	Position of a local maximum of the envelope $s_E(t)$.
f	Carrier frequency.
C	Clipping level.
$\widetilde{s}_E$	Envelop of OFDM signal after the weighting function.
u	OFDM signal After applying the windowing function.
$\hat{u}$	OFDM signal After clipping.

Δf	Frequency spacing.
P_{av}	Average power of the sampled OFDM signal.
$\mathbf{X}_m$	The m^{th} subblock
b_m	Weighting rotation factor of the m^{th} subblock.
ϕ_m	Weighting rotation angle of the m^{th} subblock.
$\mathbf{x}_m$	IDFT of $\mathbf{X}_m$.
$\mathbf{F}$	Optimum phase vector.
W	Number of rotation factors.
$\phi_m^{(k)}$	New phase factor for the m^{th} data block at the k^{th} iteration/search.
θ_m	Phase angle increment.
K	Total number of iterations predetermined.
r_m	Real-valued weighting coefficient of the m^{th} subblock.
$\mathbf{r}$	Real-valued weighting vector.

Chapter 1

Introduction

With the increasing demand on simultaneous voice, video, and data communication over the internet along with the growing interest in the design and development of the next-generation wireless communications systems, it has become necessary to develop new transmission techniques that are able to accommodate high bit-rate wideband signals and to cope well with the multipath fading of wireless channels. Multicarrier modulation (MCM) was initially proposed in 1950s for the solution of high bit-rate wireless transmission [1]. The basic idea of MCM is to divide an overall high bit-rate stream into several parallel sub-streams, each sub-stream having a much lower bit rate and being modulated with a single carrier. Orthogonal frequency division multiplexing (OFDM) is relatively a new technique that has been proposed for the realization of multicarrier modulation [2]. Unlike the traditional frequency division multiplexing (FDM) technique where each carrier uses a single frequency band and the spectrums for different carriers do not overlap, OFDM allows the spectrums from different subcarriers to be overlapped as long as these subcarriers are orthogonal, and therefore, provides a more efficient use of

spectrums and channel resources. OFDM also makes it possible to use the very powerful inverse fast Fourier transform (IFFT) for the signal generation in the transmitter [3],[4].

The OFDM technique has been investigated considerably along with its implementation issues in the last decade [5]-[8] and has found a large number of applications in military systems [9],[10] as well as in many other fields such as digital audio broadcasting (DAB), asymmetric digital subscriber lines (ADSL), and high-definition television (HDTV) terrestrial broadcasting [11]. This chapter presents a brief introduction to the multicarrier modulation system and OFDM technique, followed by the research focus and the organization of the thesis.

1.1 Multicarrier Modulation System

In a traditional single carrier transmission system as shown in Fig. 1.1, the transmitted symbols are pulse shaped by a transmit filter and then modulated with a single carrier frequency. At the receiver, the same carrier frequency is used for demodulation and a matched filter is employed to maximize the signal-to-noise ratio (SNR) of the received data. Note that in a single carrier system, the intersymbol interference (ISI) may get very severe when the data rate is large because of the short symbol interval. Also, for the wireless transmission of high bit-rate data, the multipath fading becomes considerable. In order to reduce the ISI and the impact of multipath fading on the transmission performance, it is necessary to increase the symbol duration. For this purpose, the multicarrier modulation has been proposed.

Fig. 1.1 Basic model for a single carrier system

Fig. 1.2 shows a simplified multicarrier system, where the original data stream at rate R is split into N parallel sub-streams at rate R/N. Each sub-stream is pulse shaped and modulated with a distinct sub-carrier in the transmitter. Similarly, N sub-carriers and matched filters are used at the receiver for the demodulation of the N sub-signals. Due to the fact that the symbol duration for each sub-carrier is increased by a factor of N, the ISI and the effect of multipath fading are alleviated significantly.

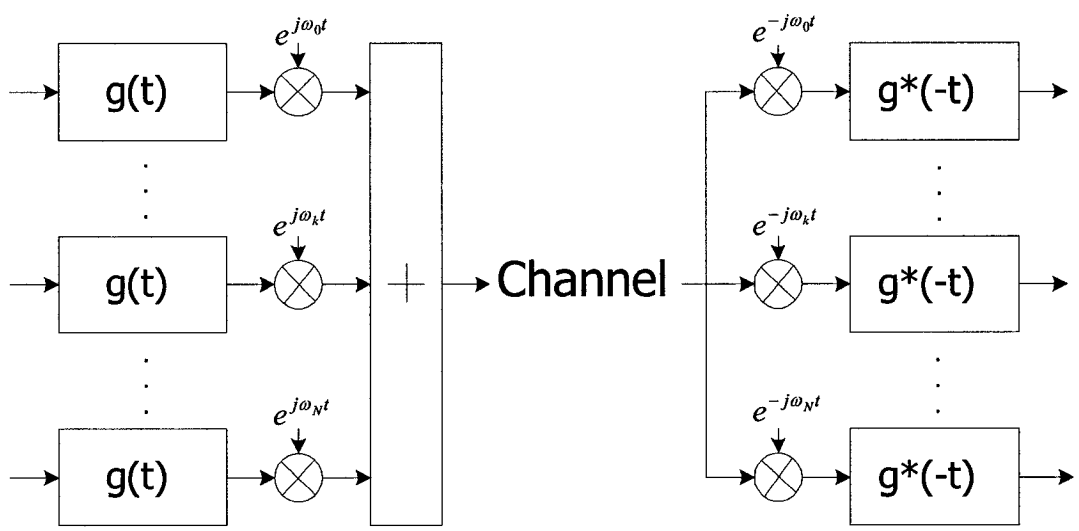

Fig. 1.2 Basic model for a multicarrier system

In a traditional multicarrier modulation system, the subcarriers should be chosen such that the spectrums of the sub-carrier signals do not overlap. As such, there is no cross-talk

(inter-carrier interference) among subcarriers. On the other hand, this scheme is not efficient in view of the spectral efficiency, since a large bandwidth is required for the transmission of non-overlapped multicarrier signals. To make a better use of the limited frequency resource, the idea of OFDM that utilizes the overlapped spectrum strategy was proposed in mid 1960's. The OFDM technique requires that the subcarriers be orthogonal to each other in order to avoid the inter-carrier interference.

1.2 OFDM Technique

The OFDM technique can be viewed as a special form of MCM with densely overlapped subcarriers. The basic idea is to spread the data to be transmitted over a large number of subcarriers, each subcarrier modulated with a much lower bit-rate data stream. These subcarriers are made orthogonal to each other by appropriately choosing the frequency spacing. In contrast to the conventional technique of using the frequency division multiplexed signals, the spectral efficiency of an OFDM signal is improved significantly.

1.2.1 Generation of OFDM Signals

An OFDM signal consists of a sum of subcarriers that are usually modulated by phase shift keying (PSK) or quadrature amplitude (QAM) signals. The equivalent complex baseband formulation of the OFDM signal can be expressed as [12]

$$s(t) = \sum_{i=-\frac{N}{2}}^{\frac{N}{2}-1} d_{i+N/2} \exp(j2\pi \frac{i}{T}(t-t_s)), \quad t_s \le t \le t_s + T$$

$$s(t) = 0, \quad t < t_s \quad or \quad t > t_s + T \tag{1.1}$$

where d_i is the transmitted symbol, N the number of subcarriers, T the symbol duration, and t_s the starting time of the OFDM symbol. Note that the final passband OFDM signal *s(t)* contains the in-phase and quadrature components that correspond, respectively, to the terms multiplied, by the cosine and sine of the desired carrier frequency (radio frequency). The formulation of baseband OFDM signal is illustrated in Fig. 1.3, where the serial-to-parallel conversion is to split the input high-rate data stream to a number of lower-rate sub-datastreams. The N multipliers are used for the modulation of the sub-datastreams with N subcarriers.

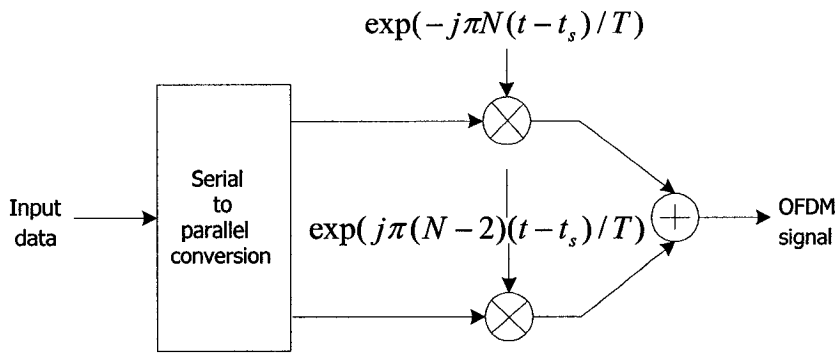

Fig. 1.3 OFDM modulator

Note that each subcarrier has exactly an integral number of cycles in one OFDM symbol interval T, and the number of cycles between the adjacent subcarriers differs exactly by one. This property accounts for the orthogonality between the subcarriers. The orthogonality is also reflected in the spectrum of an OFDM signal. Fig. 1.4 shows the spectrum of one OFDM symbol, which represents a superposition of a number of sinc functions, each corresponding to a single rectangular pulse specified by d_i and

modulated with a particular subcarrier in the time-domain. It is of interest to note that the spectrum of each subcarrier has a null at the centre frequency of any other subcarriers in the system although the spectrums from different subcarriers are overlapped. This is due to the identical frequency spacing (*1/T*) between the subcarriers and the nature of the spectrum of the rectangular pulse. In order to maintain the orthogonality between the subcarriers in an OFDM system, it is required that the receiver and the transmitter be perfectly synchronized, implying that both the transmitter and receiver have to employ exactly the same subcarrier frequencies.

In order to combat with a multipath delay in wireless channels that may cause intercarrier interference, the so-called guard interval between OFDM symbols is usually employed. In the guard interval/time, an OFDM symbol is extended by repeating the tail of that symbol. As long as the length of the guard interval is not smaller than the maximum delay caused by the multipath fading, the orthogonality between subcarriers can still be preserved.

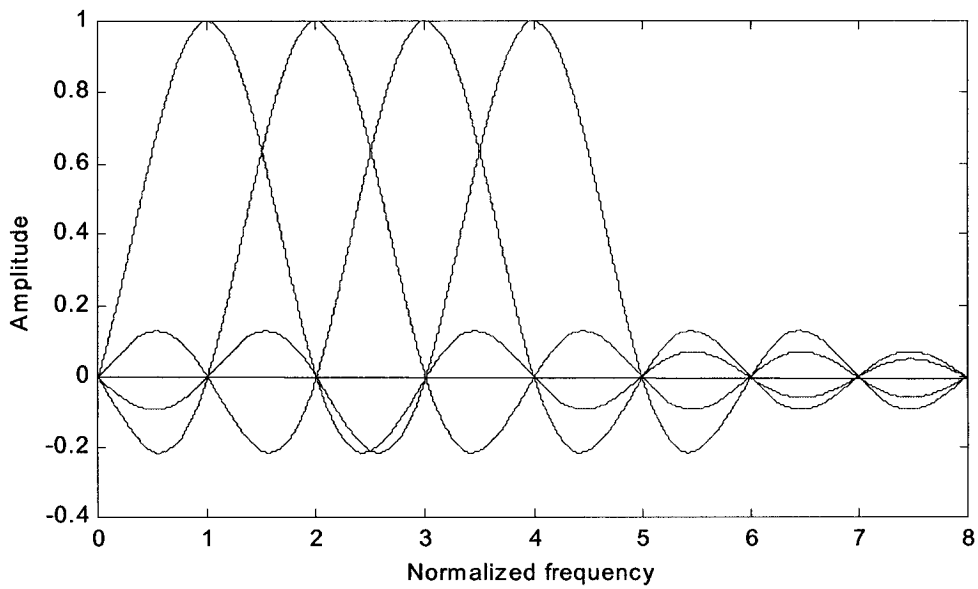

Fig. 1.4 The diagram of the orthogonality principle

1.2.2 DFT/IDFT in OFDM Systems

In a practical OFDM system, the baseband signal given by (1.1) is usually sampled and processed in a digital fashion. As a result, the inverse Fourier transform (IDFT) can readily be used to generate a discrete-time OFDM signal. This can be seen by sampling *s(t)* in (1.1) as

$$s(n) = \sum_{i=0}^{N-1} d_i \exp(j2\pi \frac{in}{N}), \qquad (1.2)$$

where N represents the number of samples per OFDM symbol T. Obviously, the IDFT can be more efficiently implemented by using the inverse fast Fourier transform (IFFT) when N is chosen as a power of 2. It is also clear that in the receiver, a DFT with the same size as the IDFT in the transmitter is required to perform the demodulation of the OFDM signal, which can therefore be implemented efficiently by utilizing the fast DFT (FFT). Fig. 1.5 shows the application of the IDFT and DFT in an OFDM system. We have assumed that the input data are first modulated with an existing quadrature modulation schemes such as QPSK (quadrature phase shift keying) and QAM (quadrature amplitude modulation), and then are converted into parallel signals. Note that a parallel-to-serial converter is required after the IFFT operation in the transmitter in order to obtain a serial discrete-time OFDM signal. In the next chapter, it will be shown that a few additional modules, pulse shaping, digital-to-analog (D/A) conversion, radio frequency modulation (baseband to passband conversion), are needed for the transmission of OFDM signals.

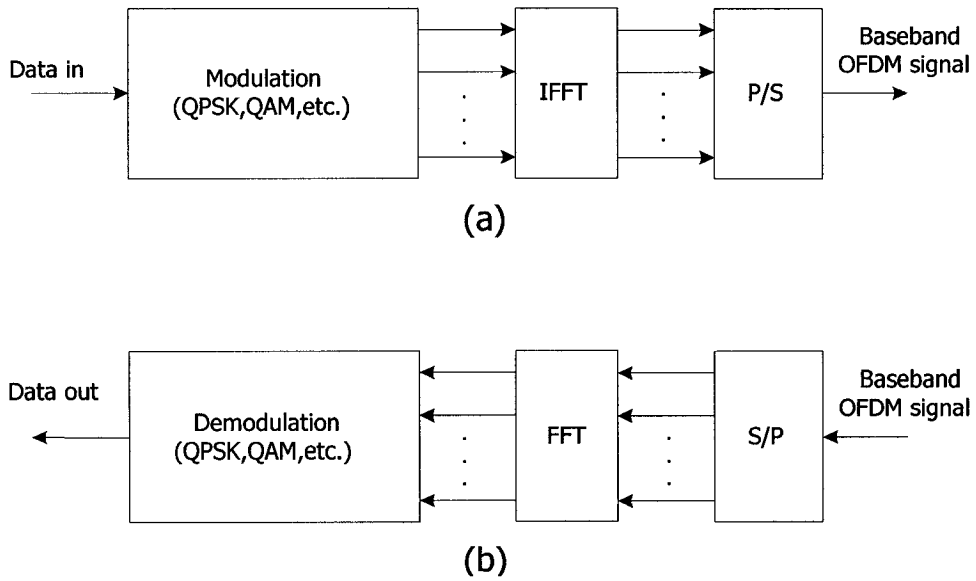

Fig. 1.5 Basic OFDM system (a) transmitter, and (b) receiver

1.2.3 Advantages and Obstacles of OFDM

Due to the spectral efficiency and the robustness to multipath fading, OFDM has found important applications in broadcasting and wireless local area networks (WLAN). It has already been adopted by IEEE 802.11a and the type-2 high performance local area network (HIPERLAN/2). It has also been proposed for the fourth generation mobile communication systems.

The major advantages of OFDM can be summarized as follows:

a. An equalizer that is normally needed in a traditional single-carrier wireless communication system can be waived in OFDM systems due to the robustness of the OFDM technique to multipath fading, thus reducing the implementation complexity of the overall system.

b. OFDM is robust against a narrowband interference, since such as an interference usually affects only a small number of subcarriers in the system.

c. OFDM is very suitable for digital broadcasting systems.

d. In relatively slow time-varying channels, it is possible to significantly enhance the capacity by adjusting the data rate for a subcarrier according to the targeted signal-to-noise ratio set for that particular subcarrier.

On the other hand, there are some obstacles that need to be overcome in the implementation of OFDM systems. The major drawbacks of OFDM are its highly sensitive to frequency error and large peak-to-average power ratio. The frequency error is usually caused by the carrier offset either in the transmitter or in the receiver. In mobile communication systems, a fast movement of mobile terminal also gives rise to a frequency offset known as the Doppler frequency shift. The frequency error causes a number of impairments, including the attenuation and rotation of the subcarriers, and the intercarrier interference (ICI). Therefore, in OFDM systems, a small frequency error can cause dramatic performance degradation. The large peak-to-average power ratio (PAPR) normally appears after the IDFT operation in the transmitter, which is critical for transmission. Unless the analog power amplifier has a very large dynamic range, the large peaks of an OFDM signal would drive it into the non-linear region, causing signal distortion and the out-of-band radiation. Therefore, it is highly desirable to reduce the PAPR. This thesis is concerned with developing techniques for reducing the PAPR and addressing the relevant implementation issues.

1.3 The Scope and Organization of the Thesis

In this thesis, the focus is on the study of several major PAPR reduction methods for OFDM signals, including the peak windowing and clipping based reduction methods, the

partial transmit sequence method, and the amplitude and phase adjustment schemes. The computational complexity and some of the implementation issues pertaining to these reduction techniques are also discussed.

The thesis is organized as follows. Chapter 2 serves as a brief overview of OFDM systems and some of the existing PAPR reduction techniques. It starts with the structure of a general OFDM system covering the transmitter, receiver and the various constituent modules, followed by a discussion of the peak-to-average power ratio and its cumulative probability distribution function. The emphasis is placed on the investigation of some typical PAPR reduction methods based on which new reduction approaches are developed in following chapters.

Charter 3 presents a PAPR reduction technique based on the windowing and clipping of the OFDM signal peaks. The idea of using either the windowing or clipping alone has been proposed in literature. However, little work has been done with regard to the joint application of the two methods and their combination schemes. In this chapter, a method that employs a peak windowing followed by clipping is proposed for the PAPR reduction. Computer simulation of the proposed method and comparison with some of the existing schemes are carried out. A modified discrete Fourier transform (DFT) based interpolation scheme is also proposed in order to improve the precision for OFDM signal interpolation.

In Chapter 4, an in-depth study of the partial transmit sequence (PTS) technique is undertaken. A framework of splitting a block of data into a number of subblocks and then applying different weights to these subblocks to achieve an optimum combination in the sense of minimizing the PAPR is established. Under this framework, a few PTS based

PAPR reduction schemes including the phase adjustment and the amplitude adjustment methods are then developed. The proposed new methods are simulated and compared with the traditional PTS method in terms of both the PAPR reduction performance and the computational complexity.

Finally, Chapter 5 concludes the thesis by highlighting the significant results from this study and providing some suggestions for future research.

Chapter 2

An Overview of PAPR Reduction Methods

2.1 Introduction

As stated in Chapter 1, a large peak-to-average power ratio (PAPR) would cause the power amplifier used in an OFDM system to be driven in the saturation region, thus leading to signal distortion. The classical remedy for this PAPR problem is to use a linear amplifier with a large dynamic range. This solution, however, imposes a stringent requirement on the analog devices in both the transmitter and receiver, and therefore, increases the cost of the system. In the last decade, many PAPR reduction methods have been proposed from the signal processing perspective. Most of these methods have focused on the discrete-time version of the baseband OFDM signal resulting from the IFFT module and attempted to decrease the instantaneous power of the signal before transmission.

This chapter starts with a brief description of typical OFDM modulation systems followed by a discussion of the issues related to the PAPR problem including the computation and distribution of the PAPR and schemes for its reduction. The emphasis is placed on the overview of some typical PAPR reduction techniques.

2.2 A Typical OFDM System

Fig. 2.1 illustrates a typical OFDM communication system that includes the transmitter, the channel and the receiver. The detailed modules in both transmitter and receiver are also shown in the diagram. The serial bit stream input to the transmitter is first converted into parallel data and then mapped to complex signals such as QPSK or QAM symbols. These parallel complex symbols are sent to the IFFT block for orthogonal modulation. The output of IFFT is then converted back to serial data stream to form the time-domain digital OFDM signal. A guard interval is normally inserted between the OFDM symbols in order to avoid the intersymbol interference (ISI) caused by the multipath distortion. The digital baseband OFDM signal with the guard interval properly inserted is converted into its analog version, and then lowpass-filtered and radio frequency (RF) modulated for transmission.

The receiver performs the inverse process of the modulation and multiplexing undertaken in the transmitter, namely, the received signal will go through the RF demodulation, analog low-pass filtering, A/D conversion, guard interval removal, serial-to-parallel conversion, and finally an FFT operation for baseband demodulation etc. In the rest of the thesis, we will restrict ourselves only to the transmitter part focusing on the PAPR reduction techniques.

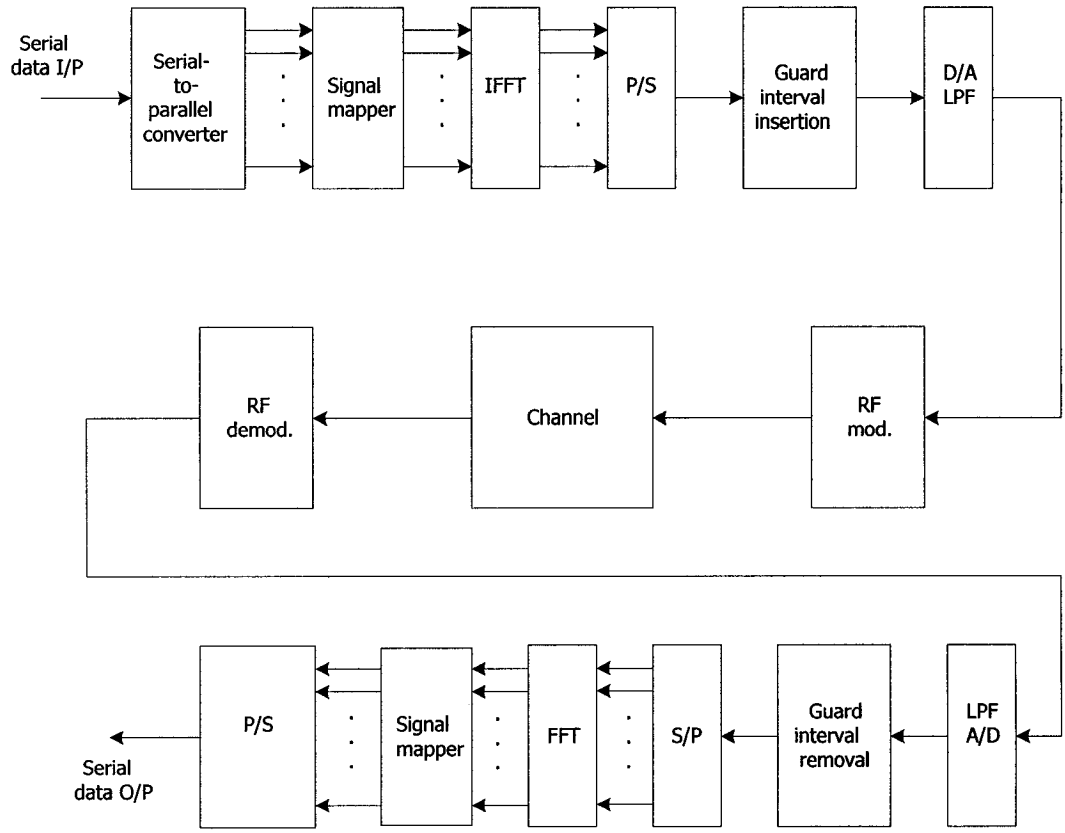

Fig. 2.1 Block diagram of a typical OFDM system

2.3 Peak-to-Average Power Ratio

The complex baseband OFDM signal in the time interval $[0, T]$ can be written as

$$s(t) = \sum_{n=0}^{N-1} a_n e^{j2\pi \frac{n}{T} t} \tag{2.1}$$

where T is the OFDM symbol duration, a_n the transmitted information symbol in the n th subchannel/subcarrier, which may be a binary number $\{\pm 1\}$ for BPSK modulation, or a complex number $\{\pm 1, \pm j\}$ for QPSK modulation, and N the number of subcarriers.

The peak-to-average power ratio (PAPR) of the OFDM signal over one OFDM symbol T is defined as [14]

$$PAPR = \frac{\max_{t\in[0,T]} |s(t)|^2}{E\{|s(t)|^2\}} \tag{2.2}$$

where $E\{\cdot\}$ denotes the expectation and $E\{|s(t)|^2\}$ represents the average power of the continuous baseband OFDM signal.

2.3.1 The Distribution of PAPR

As mentioned before, in a practical OFDM transmitter, a sequence of information bits are first mapped into the complex baseband symbols using a modulation scheme such as QPSK or QAM. Each group of N such symbols are packed into a parallel data-stream for input to the IFFT block. The time-domain OFDM signal over one interval [0, T] (usually called one OFDM symbol) is then generated by the IFFT operation as

$$s(k) = x(k) + jy(k) = \sum_{n=0}^{N-1} a_n e^{j2\pi kn/N} \qquad k \in [0, N-1] \tag{2.3}$$

We denote the OFDM signal in polar coordinates as,

$$s(k) = x(k) + jy(k) = \rho(k) e^{j\phi(k)} \tag{2.4}$$

where $\rho(k) = |s(k)| = \sqrt{x^2(k) + y^2(k)}$ is the amplitude of the kth sample of the baseband OFDM signal and $\phi(k) = \tan^{-1}(y(k)/x(k))$ is the phase. By assuming that the input information symbols are statistically independent and identically distributed (i.i.d), the real part $x(k)$ and imaginary part $y(k)$ of $s(k)$ are mutually uncorrelated [14]. From the central limit theorem, if random variables c_i ($0 \le i \le N-1$) are independent and identically distributed (i.i.d.), then the probability density function of $c = \sum_{i=0}^{N-1} c_i$, $f(c)$,

tends to be Gaussian distribution for a sufficiently large N. It follows that for a large value of N, the real and imaginary parts of $s(k)$ each can be approximated by an independent Gaussian random process with a zero-mean and variance σ_a^2, where $\sigma_a^2 = \frac{1}{2}E\left[|a_n|^2\right]$ [14]. Clearly, the amplitude $\rho(k)$ of the OFDM signal has a Rayleigh distribution [14]. We now consider the distribution of the ratio of the instantaneous power $\rho^2(k)$ to the average power $E\left[|s(k)|^2\right] = 2\sigma_a^2$. Note that $x^2(k)/\sigma_a^2$ and $y^2(k)/\sigma_a^2$ each has a chi-squared distribution with one degree of freedom. The sum $(x^2(k)/\sigma_a^2)$ + $(y^2(k)/\sigma_a^2)$ has, therefore, a chi-squared distribution with two degrees of freedom. Thus, the distribution of $\rho^2(k)/2\sigma_a^2$ can be derived using the chi-squared distribution as follows.

Let

$$u = (x^2(k)/\sigma_a^2) + (y^2(k)/\sigma_a^2). \tag{2.5}$$

The probability density function (PDF) of u can be written as

$$f_U(u) = \frac{1}{2}e^{-\frac{u}{2}}. \tag{2.6}$$

By letting $z = u/2$, we obtain the PDF of z as

$$f(z) = f_U(u)\,|_{u=2z} = e^{-z}. \tag{2.7}$$

Therefore, the cumulative distribution function (CDF) of $\rho^2(k)/2\sigma_a^2$ is given by

$$F(z) = \int_0^z e^{-v}dv = 1 - e^{-z} \tag{2.8}$$

We now consider the cumulative distribution function (CDF) of the peak-to-average power ratio over one OFDM symbol, as given by

$$PAPR = \frac{\max_{k\in[0,N-1]}|s(k)|^2}{E[|s(k)|^2]} = \frac{\max_{k\in[0,N-1]}\rho^2(k)}{2\sigma_a^2}. \quad (2.9)$$

As mentioned above, by the assumption that the N samples in one OFDM symbol are mutually uncorrelated [14],[15], the probability that the PAPR is below a specified threshold z is given by [15]

$$P(PAPR \le z) = [F(z)]^N = (1-\exp(-z))^N \quad (2.10)$$

As will be shown in the next subsection, oversampling is usually applied in the transmitter, which increases the number of samples per OFDM symbol to αN, where α is the oversampling factor. In this case, the assumption made in deriving (2.10) that the samples are mutually uncorrelated may not be true anymore. However, it seems quite difficult to come up with an exact solution for the distribution of the peak power. The effect of oversampling is usually approximated by adding a certain number of extra independent samples [15]. Thus, the cumulative distribution of the PAPR in the case where oversampling is applied is modified as

$$P(PAPR \le z) = (1-\exp(-z))^{\alpha\cdot N} \quad (2.11)$$

2.3.2 Oversampling Issue

The actual PAPR should be computed based on the analog baseband OFDM signal. However, the IFFT module yields a discrete-time signal with the information-symbol

spaced samples. This discrete-time signal is usually upsampled and converted into its analog version for transmission. The upsampled signal should be used for the calculation of PAPR in order to achieve a better approximation of the actual PAPR. In OFDM systems, the upsampling process can be implemented in the IFFT block by using a larger size, for example a size of 4N, for the IFFT. Therefore, in an OFDM transmitter, an oversized IFFT is often employed, giving an over-sampled time-domain signal directly. This is the so-called oversampling procedure. We will revisit this issue in Chapter 3.

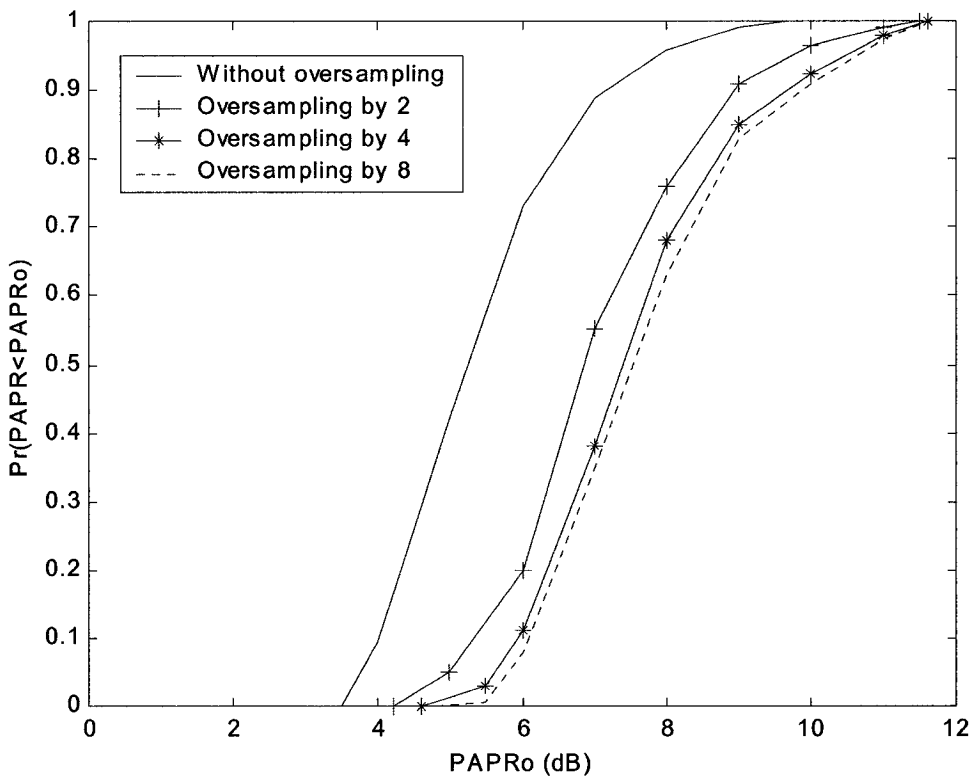

Fig. 2.2 Distribution of the PAPR with different oversampling factors

Fig. 2.4 shows the simulation results for the cumulative probability distribution of PAPR for different oversampling factors. It is clear that if the signal is oversampled by a factor of 2, a much more accurate PAPR can be obtained in comparison to the case without using oversampling. When the oversampling factor is increased to 4, a further improvement in the accuracy is attained but the improvement is not as much as it is for the rate increase from non-oversampling to oversampling by 2. It should be mentioned that a further increase in the sampling rate, such as a factor of 8 or 16, would not lead to a considerable improvement in the accuracy while it would in a higher computational burden. Hence, oversampling by a factor of 4 is considered throughout this thesis.

2.4 The Existing PAPR Reduction Approaches

As described in the previous section, a large PAPR would drive the analog power amplifier to saturation, producing interference among the subcarriers and corrupting the signal spectrum. In order to avoid the power amplifier to enter into the non-linear region, one may reduce the average power of the transmitted signal. However, reducing the average power level too much will bring down the signal-to-noise ratio and hence, degrade the bit error rate (BER) performance of the system. Therefore, it is preferable to resolve the PAPR problem by means of reducing the peak power of the signal. Many PAPR reduction techniques have been proposed in literature. They can be broadly divided into three categories. The so-called signal distortion techniques [15]-[18] belong to the first category, which simply reduce or clip the peak amplitudes of a signal at the expense of introducing a slight distortion to the spectrum of the signal. The second category consists of the techniques that use a special coding sequence to generate OFDM

symbols meeting the target PAPR [19]-[20]. In the third category, the technique used is to scramble each OFDM symbol with different scrambling codes and then select the sequence with the lowest PAPR for transmission. In this section, a brief overview of the PAPR reduction techniques belonging to the three categories is presented.

2.4.1 Signal Distortion Techniques

Even though the PAPR of an OFDM signal may be quite large, the high magnitude peaks occur very rarely and most of the signal power is dependent mainly on the signal samples with low amplitude. Therefore, the amplitude peaks may be reduced or clipped without introducing a severe distortion in the signal.

a) Clipping

The simplest distortion technique is the clipping or hard-limiting method [16], which limits the instantaneous signal peak to a preset threshold prior to sending the signal to power amplifier. Depending on the level of threshold, the signal is distorted more or less severely and the BER performance is degraded accordingly. Although a lowpass filter can be used along with the clipping to alleviate the spectral splattering effect, sometimes the problem of peak regrowth may occur after the lowpass filtering.

b) Peak windowing

Different from the clipping method that hard-limits the large signal peak to a preset level, in the peak windowing method, a window is applied to a region where there exist large peaks. The window function is multiplied with the signal in such a way that the signal peaks fall in the valley or center of the window while the signal samples with lower amplitudes align themselves with the large amplitude segment of the window function. The most commonly used window functions include the Hamming window, and the

Kasier window. It is known that the peak windowing scheme exhibits some good properties such as it is very simple to implement and is independent of the number of subcarriers.

c) Peak cancellation

The peak cancellation method was first introduced in [21]. In this method, a reference function that has approximately the same bandwidth as the transmitted signal is properly designed. The reference function is time-delayed, scaled and then subtracted from the signal portion where peaks occur in order to cancel signal peaks. Fig. 2.3 shows the block diagram of an OFDM transmitter with peak cancellation module, which contains a peak power/amplitude detector, a comparator for the comparison of the peak power with a prescribed threshold as well as a scaler that rescales the peak and surrounding samples.

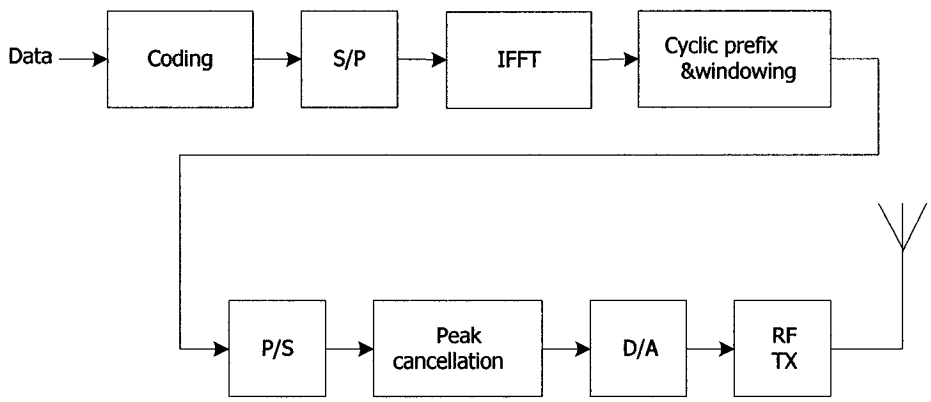

Fig. 2.3 OFDM transmitter with peak cancellation

Peak cancellation can also be carried out immediately after the IFFT operation [22]. Fig. 2.4 shows a detailed diagram for this cancellation scheme. In this scheme, an impulse is generated once a signal peak has been detected. The impulse is first low-pass

filtered and then the output is used as a reference sequence. The FFT and the IFFT blocks are readily employed to perform the low-pass filtering in the discrete frequency domain. Clearly, after the FFT computation, the low-pass filtering is simplified as a setting-to-zero operation, namely, the outputs of the IFFT that correspond to the frequencies larger than the highest subcarrier is set to zero.

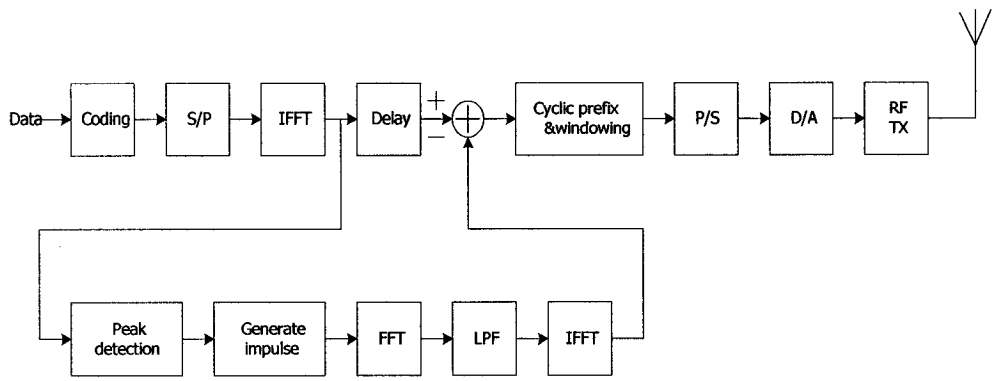

Fig. 2.4 Peak cancellation using FFT/IFFT to generate a cancellation sequence

2.4.2 Coding Technique

In coding techniques, the OFDM symbols for which the PAPR is below a desired threshold are coded using a coding sequence. The smaller the desired PAPR threshold, the smaller code rate that can be achieved. In [23], a code of rate ¾ has been found through an exhaustive search for the case of eight subchannels, which gives a maximum of 3 dB. The Golay complementary sequence has been found to be a very good candidate [23]-[25]. It has a strong auto-correlation property, namely, the correlation of the sequence with its delayed version is zero. It has been shown in [26] that the correlation property of the complementary sequence translates to a reduction of the PAPR by 3 dB

when the sequence is used to modulate an OFDM signal. In [27], a specific subset of Golay codes along with the associated decoding scheme has been proposed for coding the OFDM symbols. Based on this work, Golay codes were later implemented in a prototype 20 Mbps OFDM mode, for the European magic WAND project [28]. Detailed studies on the coding properties of the Golay sequences, the determination of the code set size and the relation to the Reed-Muller codes can be found in [29].

2.4.3 Symbol Scrambling

The basic idea of symbol scrambling is to scramble the input OFDM symbols by using a number of scrambling sequences. The output scrambled signal corresponding to the smallest PAPR is then transmitted. A number of symbol scrambling methods have been proposed [30]-[33]. Some of these schemes give a very low PAPR but they are often difficult to be implemented in practice. The 'selected mapping' and the 'partial transmit sequences' methods have been proposed as a more practical solution [31],[32]. The difference between these two methods is that the former applies an independent rotation to each subcarrier, while the latter applies a scrambling code only to each group of subcarriers.

a) Selected mapping (SLM)

The selected mapping (SLM) scheme was first proposed in [31]. The idea is to choose one particular signal out of the M signals obtained from the scrambling of the OFDM signal, which has the lowest PAPR.

In order to obtain M scrambled signals, define the M distinct vectors as

$$\mathbf{P}^{(m)} = [\mathbf{p}_1^{(m)} \ldots \mathbf{p}_N^{(m)}] \tag{2.12}$$

with

$$\mathbf{p}_{\mu}^{(m)} = e^{j\phi_{\mu}^{(m)}}$$

where $\phi_{\mu}^{(m)} \in [0,2\pi), (\mu = 1,...,N, m = 1,...,M)$. Denoting the μ-th subcarrier as $V[\mu]$, after mapping, the subcarrier signal can be written as

$$V^{(m)}[\mu] = V[\mu] \cdot e^{j\phi_{\mu}^{(m)}}, \quad (\mu = 1,...,N, m = 1,...,M). \tag{2.13}$$

Then each of the M OFDM frequency-domain sequences is transformed using the IFFT into the time-domain signal and the one with the lowest PAPR is selected for transmission. To recover the original OFDM symbols, the receiver has to know as to which vector $\mathbf{P}^{(m)}$ has been selected for PAPR reduction. A straightforward method is to transmit the index **m** of the vector as side information to the receiver. This method can be used for an arbitrary number of carriers and for any signal constellation. It provides a significant reduction in PAPR with a moderate additional complexity.

Fig. 2.5 shows the basic structure for the SLM method, where the 'Mapping' block is to perform the conversion from the binary data stream to a complex symbol stream such as QPSK signals, and each of the phase adjustment blocks is to implement the mapping/rotation of each subcarrier as required by (2.13). The 'No adjustment' block is included as a result of considering the original OFDM symbol to be a possible candidate for the output for which no PAPR reduction is necessary. The major computational burden of the SLM method is in the computations carried out by the M IFFT blocks.

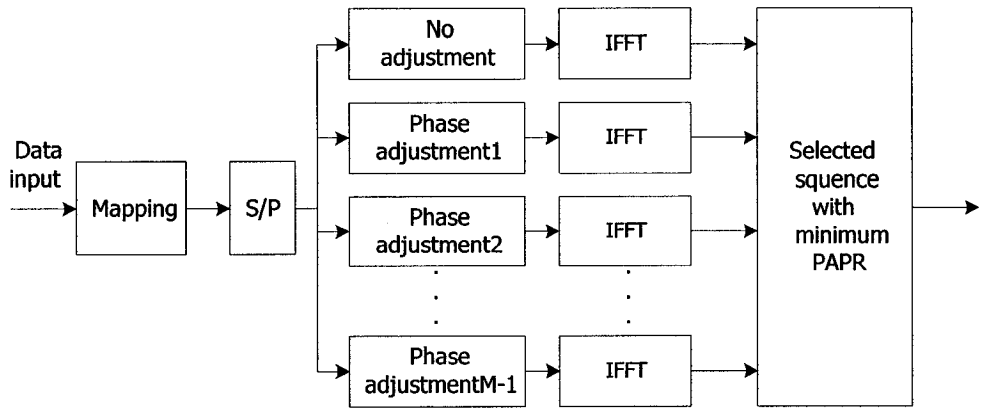

Fig. 2.5 Block diagram for the SLM method

b) Partial transmit sequences (PTS)

In the PTS method, each block of data input to the inverse discrete Fourier transform (IDFT) is divided into a number of disjoint subblocks and each subblock, after zero padding, computes an independent full-size IDFT. The outputs of these IDFT's are then properly combined such that a low PAPR is achieved.

Let $\mathbf{A}$ be the input data vector to the IDFT block. It can be split into V sub-vectors, each sub-vector being appropriately padded with zeros to form an N-dimensional vector. Then, $\mathbf{A}$ can be rewritten as

$$\mathbf{A} = \sum_{v=1}^{V} \mathbf{A}^{(v)} \tag{2.14}$$

where any two of $\mathbf{A}^{(v)}$'s (v=1,2,..., V) are orthogonal, i.e., they disjointly contain the elements of $\mathbf{A}$. By multiplying each vector $\mathbf{A}^{(v)}$ by a rotation factor $b^{(v)} = e^{j\phi^{(v)}}$, $\phi^{(v)} \in [0, 2\pi)$, we obtain the combination of the rotated vectors as given by

$$\overline{\mathbf{A}} = \sum_{v=1}^{V} b^{(v)} \cdot \mathbf{A}^{(v)} \tag{2.15}$$

The coefficient set $\{b^{(v)}, v = 1,...,V\}$ is usually called the side information, which is known for a particular OFDM symbol and should be transmitted to the receiver. Note that this coefficient set or rotation factor may be different from symbol to symbol, and therefore, needs to be updated for each OFDM symbol. The IDFT of $\overline{\mathbf{A}}$ can then be written as

$$\overline{\mathbf{a}} = \sum_{v=1}^{V} b^{(v)} \cdot IDFT\{\mathbf{A}^{(v)}\} = \sum_{v=1}^{V} b^{(v)} \cdot \mathbf{a}^{(v)} \tag{2.16}$$

where $\mathbf{a}^{(v)}$ represents the IDFT of $\mathbf{A}^{(v)}$. The PTS method is to find the optimum rotation factor $\overline{b}^{(v)}$ such that the PAPR is minimized, yielding the optimum transmit sequence as given by

$$\overline{\mathbf{a}} = \sum_{v=1}^{V} \overline{b}^{(v)} \mathbf{a}^{(v)} . \tag{2.17}$$

For computational simplicity, the first element $b_{\mu}^{(1)}$ in the rotation vector is always set to 1. Furthermore, the rotation factors are normally limited to some constant values such as $\{\pm 1, \pm j\}$, which correspond to a set of rotation angles $\{0, \pi/2, \pi, 3\pi/2\}$. In this case, one just needs to find the optimum combination of these parameters. However, depending on the number of the subblocks, an exhaustive search for these phase values may be computationally expensive.

Fig. 2.6 shows the implementation structure for the PTS method commonly used in the OFDM transmitter. The PTS method can be viewed as a variation of the SLM method, in which the phase rotation is based on each subblock instead of the individual subcarrier. The PTS method has a slightly higher computational complexity than the SLM method, yet it provides a better performance in decreasing the PAPR.

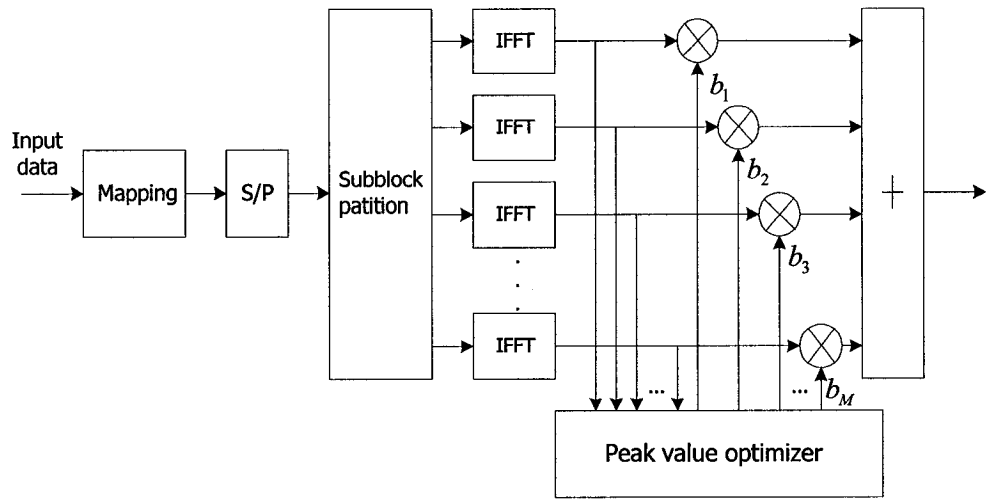

Fig. 2.6 Block diagram for the PTS method

2.5 Conclusion

In this chapter, the structure of a typical OFDM system consisting of the transmitter, receiver and the relevant modules has been presented. Based on the transmitter structure, the PAPR has been introduced and analyzed, resulting in a closed-form expression for the cumulative distribution function of the PAPR. The theoretical result for the distribution of PAPR has been simulated to show its deviation from the actual distribution.

The necessity of using the oversampling strategy for the output of the IFFT has been briefed. It has been pointed out that oversampling the time-domain OFDM signal by a factor of 4 gives the best trade-off between the computational complexity and the

precision for the evaluation of the PAPR. The emphasis in this chapter has been on the issue pertaining the PAPR reduction. Some of the major techniques existing in literature for the reduction of PAPR have been reviewed, including the signal distortion methods, coding techniques and scrambling methods. The variations of these methods and their features have also been discussed, providing a motivation for the development of some new PAPR reduction schemes to presented in following chapters.

Chapter 3

PAPR Reduction Using Peak Windowing along with Clipping

3.1 Introduction

Even though the PAPR of an OFDM signal could be quite large, amplitudes with a large peak value may appear infrequently. The simplest way to reduce the PAPR is to clip the high peak amplitudes by employing the signal distortion techniques such as clipping [16] and peak windowing [15],[17]. These techniques are very easy to implement and are independent of the number of subcarriers. However, the clipping technique usually produces a large out-of-band radiation which leads to a poor spectral efficiency, whereas the peak windowing method affects more signal samples, and therefore, degrade the BER performance. Considering these drawbacks, a new distortion scheme that combines the peak windowing with clipping is proposed in this chapter as a compromise between the out-of-band radiation and the in-band distortion. The proposed scheme is applied to the interpolated time-domain OFDM signal, where the interpolation is realized using a modified oversized IDFT.

In Section 3.2, a joint peak windowing and clipping scheme for PAPR reduction is proposed. The commonly used IDFT interpolation method is modified for our scheme in order to improve the interpolation precision. Section 3.3 shows simulation results for the proposed combination scheme, namely, the out-of-band radiation and the BER performance. A comparison of the proposed scheme with some of the existing distortion techniques is also provided in this section. In section 3.4, an analysis is carried out to compare the complexity of the proposed scheme with that of the existing distortion methods. Finally, in Section 3.5, we present the conclusion for this chapter by summarizing some of the research results.

3.2 The Proposed PAPR Reduction Method

Fig. 3.1 depicts the block diagram of the proposed OFDM transmitter. The randomly generated binary sequence is first mapped to QPSK symbols. Then, an oversized IDFT is used to obtain the interpolated OFDM signal. The peak windowing combined with clipping is employed to eliminate the peak values of the power of the interpolated signal for PAPR reduction. As in the conventional OFDM systems, the cyclic prefix padding and D/A conversion are also needed. In our study, however, we concentrate on the IDFT interpolation and the PAPR reduction.

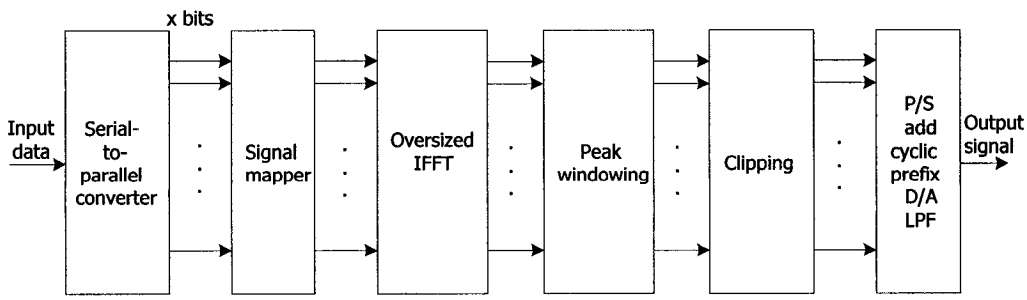

Fig. 3.1 Block diagram for the proposed PAPR reduction scheme

3.2.1 Signal Mapping

The incoming serial data stream is first converted into parallel stream and appropriately formatted according to the word size required for transmission; for instance, 1 bit/word for BPSK and 2 bits/word for QPSK. In this study, the data to be transmitted are mapped into a QPSK symbol stream. The QPSK modulation is a bandwidth-efficient scheme and it is widely used in digital transmission systems. It has also been adopted in the third generation wireless communication systems. The QPSK modulator is shown in Fig. 3.2 and the corresponding signal constellation diagram in Fig. 3.3.

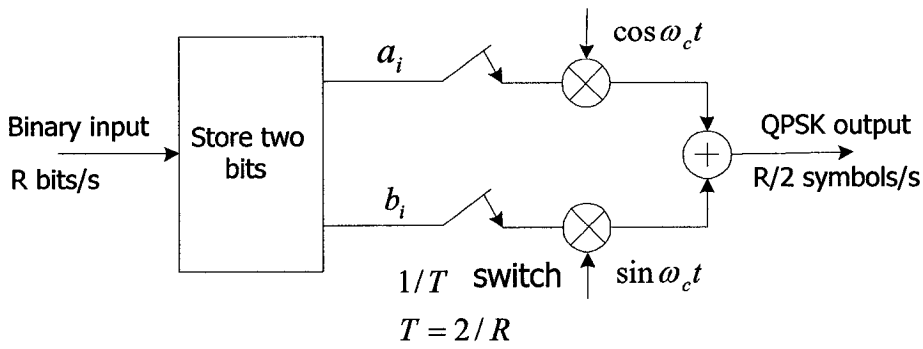

Fig. 3.2 QPSK modulator

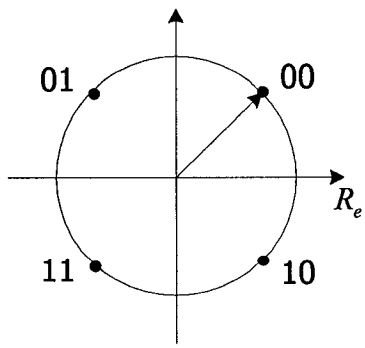

Fig. 3.3 QPSK signal constellations

3.2.2 IDFT Interpolation

An interpolation between the successive samples of a sequence is often required in OFDM systems. It is well known that the DFT/IDFT can be used for signal interpolation [35]-[37]. The interpolation of an OFDM baseband signal can be performed by inserting $N(M-1)$ zeros in the middle of the input vector to DFT/IDFT, where M is the interpolation factor. This results in a trigonometric interpolation of time domain signal at the output of IDFT. In [37], an oversized IDFT has been used to interpolate the OFDM baseband signal. However, the middle value of the input vector, i.e., the spectral component at the Nyquist frequency $N/2$ has not been used in [37]. This omission may lead to a large interpolation error. In what follows, we will make use of the middle value to improve the interpolation precision.

Assume that $s(i)=s(t)|_{t=iT}$ (i=0,1,2,...,N-1) represents the sampled version of a continuous-time signal $s(t)$, and its N-point DFT is denoted as $S(k)$. The signal $s(i)$ is to be interpolated by a factor of M. One can perform the interpolation by appropriately expanding the frequency-domain N-point sequence $S(k)$ to a sequence of length $L=MN$, and then computing the L-point IDFT. Let this new sequence be given by

$$V(k)=\begin{cases} S(k) & k=0,1,...,N/2-1, \\ 0.5S(k) & k=N/2, \\ 0 & k=N/2+1,...,L-N/2-1, \\ 0.5S(k-L+N) & k=L-N/2, \\ S(k-L+N) & k=L-N/2+1,...,L-1. \end{cases} \tag{3.1}$$

Note that in regular DFT interpolation, the coefficient *S(k)* is set to be zero at *k=N/2* and *k=L-(N/2),* implying that the DFT coefficient *S(N/2)* is never used. In our scheme, however, *0.5S(N/2)* is assigned to *V(N/2)* and *V(L-N/2)* considering that *S(N/2)* corresponds to the highest frequency component.

Using (3.1), the inverse DFT of *V(k)* can be expressed as

$$\begin{aligned} v(n) &= \sum_{k=0}^{L-1} V(k) e^{j2\pi nk/L} \\ &= \sum_{k=0}^{N/2-1} S(k) e^{j2\pi nk/L} + S(N/2)\cos(\pi n/M) \\ &\quad + \sum_{k=L-N/2+1}^{L-1} S(k-L+N) e^{j2\pi nk/L} \qquad (n = 0,1,\ldots,L-1) \end{aligned} \tag{3.2}$$

where $j = \sqrt{-1}$. Note that if M is even, as normally assumed for IDFT interpolation, then $S(N/2)\cos(\pi n/M) = 0$, for *n=M/2, 3M/2,....* Also, it can easily be verified that $v(Mi) = s(i)$, i=0,1,2,..., N-1. In other words, the values of the original samples in *s(n)* remain unchanged in the interpolated sequence, implying that the reconstruction error is zero at the original sampling instants.

The absolute value of the error between the original and the reconstructed signals can be written as

$$e(n) = |s(n) - v(n)| \tag{3.3}$$

where $s(n) = s(t)\,|_{t=\frac{T}{L}n}$. Define the total interpolation error as

$$\hat{e} = \sum_{n=1}^{L} e(n) \Big/ L. \tag{3.4}$$

In order to illustrate the interpolation precision, let us consider a sinusoidal signal,

$$s(t) = \cos\left(\frac{2\pi ft}{N} + \phi\right) \tag{3.5}$$

Fig. 3.4 shows the error sequence plots for the proposed scheme and the interpolation method presented in [37] that sets $V(\frac{N}{2})$ and $V(L-\frac{N}{2})$ to zero. In our simulation, we have chosen f=4.5, N=64, ϕ =-π/3, and M=8. Clearly, the proposed interpolation scheme gives a smaller error. We have also found the total interpolation error $\hat{e}$ =0.0127 for the proposed method and $\hat{e}$ =0.0141 for the scheme in [37]. It is worth mentioning that the interpolation performance does not depend on the parameters chosen for (3.5). In general, our method yields a better interpolation precision.

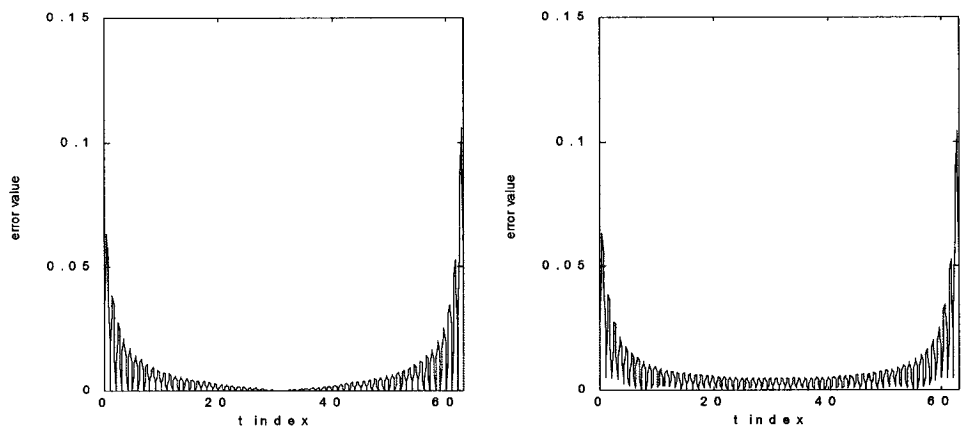

(a) (b)

Fig. 3.4 Interpolation error plots for two DFT-based interpolation schemes (a) The proposed scheme, and (b) The scheme presented in [37]

3.2.3 Joint Peak Windowing and Clipping

The time-domain OFDM signal can be written as

$$s(t) = \sum_{n=0}^{N-1} a_n e^{j2\pi \frac{n}{T} t} \qquad 0 \le t \le T \tag{3.6}$$

where a_n is the transmitted symbol in the nth subchannel, N the number of subcarriers, and T the original symbol period. The envelop of the OFDM signal is denoted as

$$s_E(t) = |s(t)| \tag{3.7}$$

Assuming that the information symbols are statistically independent and identically distributed (i.i.d), the real and imaginary parts of the sampled version $s(n)$ of $s(t)$ are uncorrelated. For a considerably large N, both the real and the imaginary parts of $s(n)$ approach a Gassian distribution with a zero mean and variance σ_s^2 , where $\sigma_s^2 = \frac{1}{2} E[|a_n|^2]$. Thus, the amplitude envelop s_E has a Rayleigh distribution with the probability density function (PDF) given by

$$p(s_E) = \begin{cases} \dfrac{s_E}{\sigma_s^2} e^{-s_E^2/(2\sigma_s^2)}, & s_E \ge 0 \\ 0, & otherwise. \end{cases} \tag{3.8}$$

The PAPR of the OFDM signal can be calculated as

$$PAPR = \max s_E^2(t) / E[s_E^2(t)] \tag{3.9}$$

We now propose a joint peak windowing and clipping method for the reduction of the PAPR given by (3.9). In the combination scheme, we first search for the envelope amplitudes of the OFDM signal. When the amplitude exceeds a threshold, a weighting window function is applied to the envelope of the OFDM signal to eliminate the peak amplitude. Then, the remaining peak values are clipped with hard limiting.

A) Peak Windowing

The basic idea of peak windowing is to multiply the envelope $s_E(t)$ with a weighting function. Thus, we have

$$\tilde{s}_E(t) = s_E(t) \cdot f(t) \tag{3.10}$$

where the weighting function is given by

$$f(t) = 1 - \sum_{t=t'} \alpha \cdot w(t - t') \tag{3.11}$$

where *w(t)* is the window function, t' denotes the position of a local maximum of the envelope $s_E(t)$ and the weighting coefficient α is chosen as

$$\alpha = (s_E(t) - C)/s_E(t) \tag{3.12}$$

In (3.12), the constant C represents the clipping level, which is a prescribed threshold used to eliminate the peak amplitudes. In this study, we use the Hamming window function for *w(t)* in (3.11), namely,

$$w(t) = \begin{cases} 0.54 + 0.46\cos(2\pi t/T), & 0 \le t \le T \\ 0, & othetrwise \end{cases} \tag{3.13}$$

As a matter of fact, other windows such as Hanning and Kaiser windows [15] may be employed provided that they have a good spectral property. It is seen from simulations that the Hamming window function yields a slightly better performance.

B) Clipping

After applying the windowing function, the OFDM signal can be written as

$$u(t) = \tilde{s}_E(t) \cdot e^{j\phi} \tag{3.14}$$

where $\phi = \arg\{s(t)\}$. The signal *u(t)* is then clipped as [38]

$$\hat{u}(t) = \begin{cases} u(t), & |u(t)| \le C \\ C \cdot e^{j\phi}, & |u(t)| > C \end{cases} \tag{3.15}$$

where C represents the clipping level, i.e., the signal u(t) should be hard-limited if it exceeds this level. As a result, the PAPR is reduced to

$$PAPR = C^2 / E[|\hat{u}(t)|^2] \tag{3.16}$$

The clipping level C plays an important role in reducing the PAPR. The smaller the value of C, the larger the reduction of the PAPR. However, a small value of C means a degradation of the BER performance.

3.3 Simulation Results

This section shows the simulation results for the proposed scheme of peak windowing plus clipping. Different choices for the window function, the length of the window and the clipping level for the proposed scheme are considered. A comparison of the proposed scheme with some of the existing PAPR reduction methods in terms of the power spectral density of the OFDM signal and the BER performance of the OFDM system is also carried out.

3.3.1 Assumption Used for the Simulation

In our simulation, we consider an OFDM system with 256 subcarriers. The quadrature-phase shift-keying (QPSK) modulation is employed for the binary input sequence. The modulated QPSK symbols are then passed through an oversized IFFT module with an oversampling factor of 4 to implement the OFDM modulation. As mentioned earlier,

oversampling is often applied in a practical communication system and it allows a more accurate computation of the PAPR. Oversampling by a factor of 4 is sufficient to capture signal peaks [39]. Increasing the oversampling rate further does not result in a significant improvement of the performance, yet it increases the system complexity to a considerable degree. As for the choice of the window function, theoretically, the window should be as narrowband as possible in order to preserve the spectrum of the transmitted OFDM signal. On the other hand, a window with a very short length requires more multiplications and more searches. Through extensive simulation experiments, we have found that a length of 9 is an appropriate choice for the window function. In addition, we assume that the power is equally distributed among subcarriers, which is a typical configuration for OFDM systems. The channel is assumed to be AWGN without multipath fading. The parameter values and the system configuration used for the simulation are summarized in Table 3.1.

Table 3.1 OFDM system parameters used for the simulation

Parameter	Configuration
Carrier modulation scheme	QPSK
FFT size	1024
Number of carriers	256
Oversampling rate	4
Window length	9
Link	Synchronous downlink
Channel model	AWGN

To study the BER performance of the proposed scheme, the Monte Carlo simulation is used. Although this method is not suitable for the computation of a very low BER because of the significantly large computer time, it is widely used in the simulation of wireless mobile systems. For the BER simulation of the OFDM system, as stated above, the channel is modeled as an additive white Gaussian noise (AWGN) in this study.

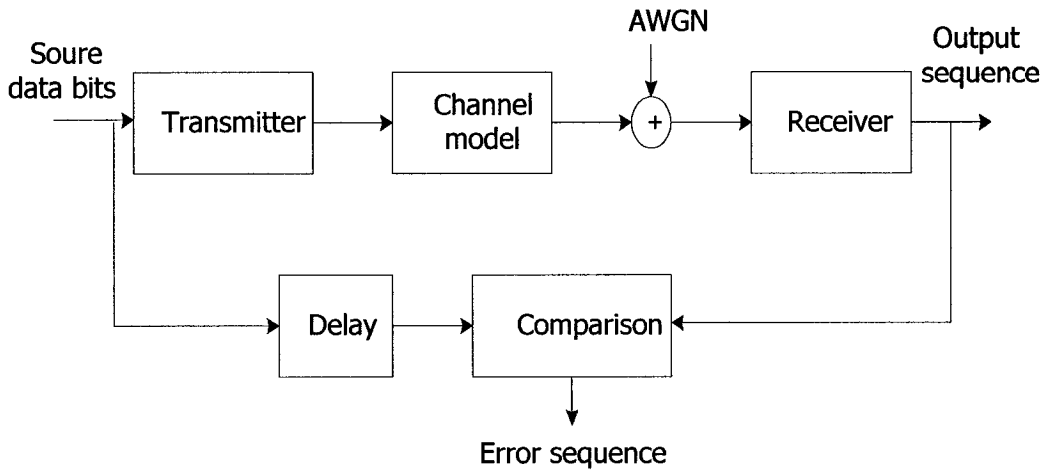

Fig. 3.5 Monte Carlo BER simulation model

Fig. 3.5 shows the implementation diagram for the Monte Carlo method. The source data are compared with the detected data in order to find the number of bit errors. The BER is calculated by dividing the number of error bits by the number of data bits.

3.3.2 Comparison of the Proposed Scheme with the Clipping Method

We would first like to examine the power spectral density (PSD) of the OFDM signal after PAPR reduction. Fig. 3.6 shows the PSD result obtained from the proposed method where three Hamming windows with different lengths (L=5, 9 and 15) are used to compare the PSD with the non-distorted case without using the peak windowing. One can see that the out-of-band radiation occurs when peak windowing is applied, and gets worse

as the window length decreases. On the other hand, using a longer window function would affect more signal samples, and hence, degrade the BER performance. As a consequence, a compromise between the BER and the out-of-band radiation should be achieved by choosing a proper window length. From simulation results, it is found that L=9 is an appropriate choice.

A comparison of the proposed scheme with the conventional clipping method in terms of the PSD of the PAPR-reduced OFDM signal is depicted in Fig. 3.7. Fig. 3.7 (a) shows the result of using the clipping method alone, whereas Fig. 3.7 (b) gives the results of the proposed method of using the joint peak windowing and clipping together. It is obvious from these two plots that the out-of-band spectrum drops more rapidly by employing the proposed scheme than that using the conventional clipping technique. Therefore, the PSD performance of the OFDM signal is significantly improved by applying the proposed scheme.

Fig. 3.8 shows the PSD of the OFDM signal after the PAPR reduction employing the Hamming and Hanning windows. We see that these two windows actually yield a very similar performance in respect of the out-of-band radiation. However, Hamming window is slightly better in view of its influence on the original signal spectrum outside the desired frequency band.

As mentioned earlier, the clipping level C is an important parameter that affects PAPR reduction performance. A normalized clipping level called the clipping ratio (CR) is defined as the ratio of the clipping level to the mean power of the unclipped OFDM baseband signal [37]. Fig. 3.9 shows the BER vs. SNR plots for different CR values. The linear values of BER with different CR and SNR values are also given in Table 3.2,

where the SNR is the average value over all the subchannels. Obviously, a larger clipping ratio implies that less peak amplitudes are clipped and therefore leads to a better BER performance. However, a large clipping ratio implies a large-amplitude OFDM signal, which as explained earlier, could be detrimental to the linear operation of the analog amplifier.

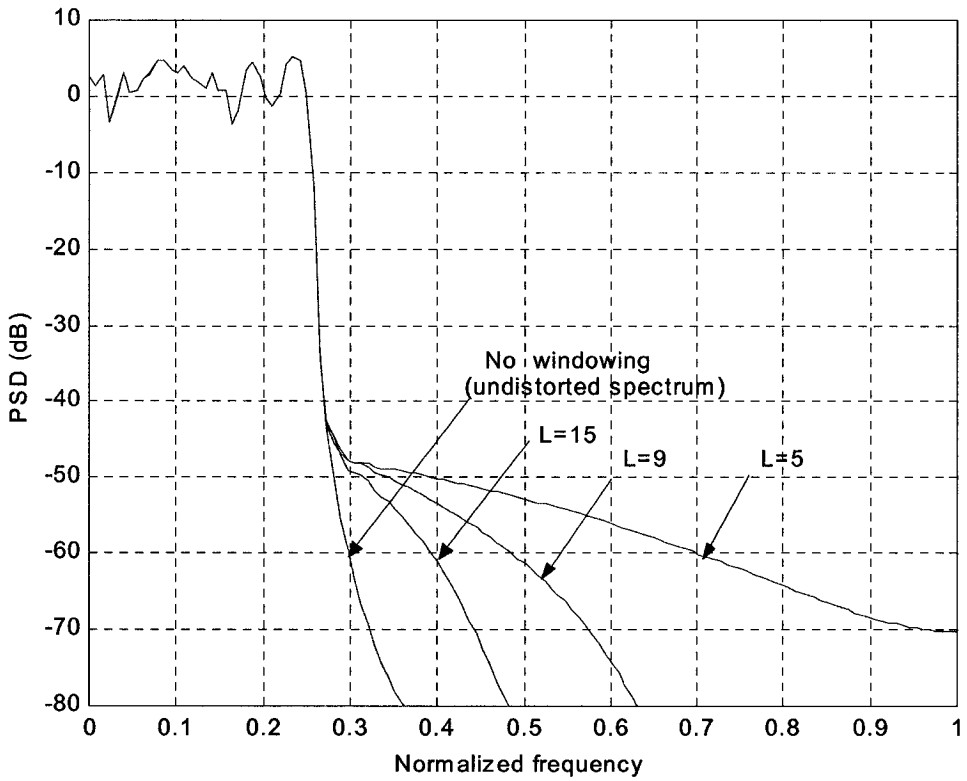

Fig. 3.6 The PSD of OFDM signal after peak windowing with different window lengths

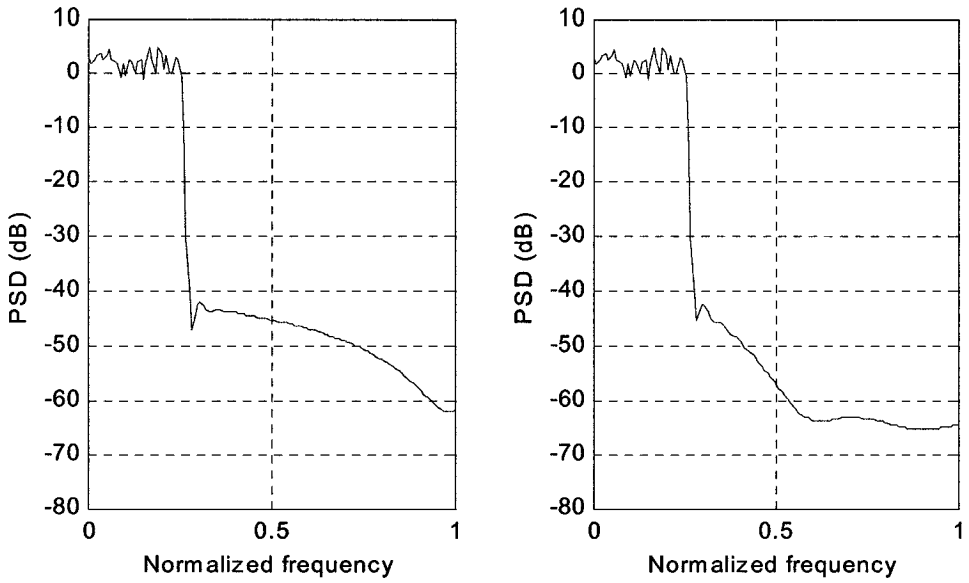

Fig. 3.7 The PSD of OFDM signal after PAPR reduction by using (a) the clipping technique, and (b) the proposed scheme

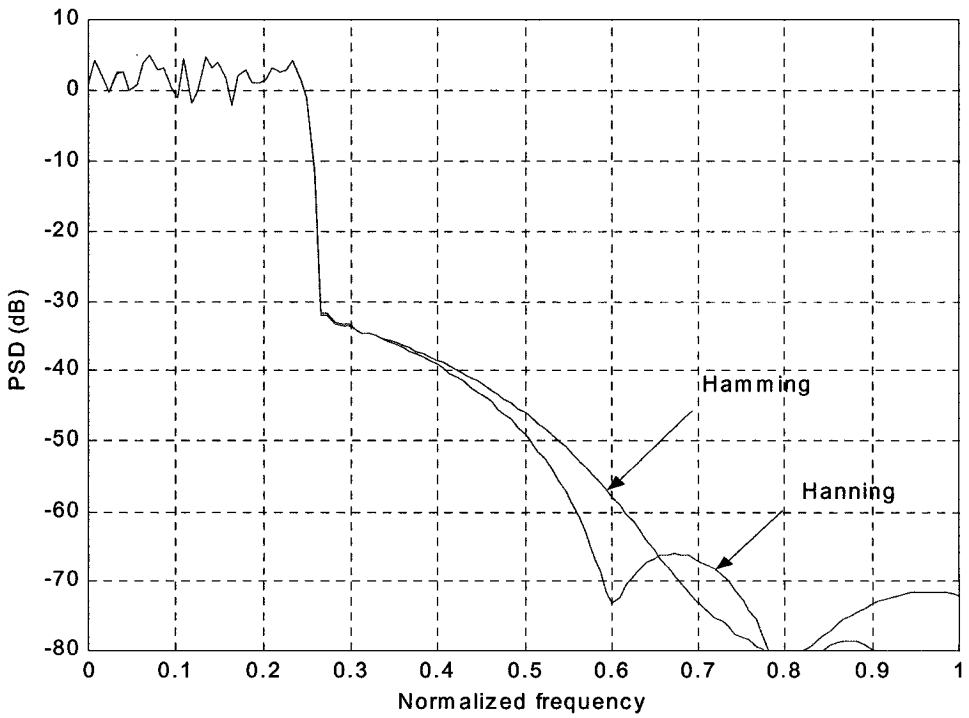

Fig. 3.8 The PSD of OFDM signal using different windows

As shown in Fig. 3.10, the BER performance of the proposed method is also compared with that of the conventional clipping technique. In this simulation, CR is set as 1.8. It is seen that the BER degradation caused by the proposed method is about 0.6 dB only in comparison to the conventional clipping method at 10^{-4} level. Table 3.3 lists the BER values for the proposed method and the conventional clipping technique when SNR is set to be 10 dB and 13 dB.

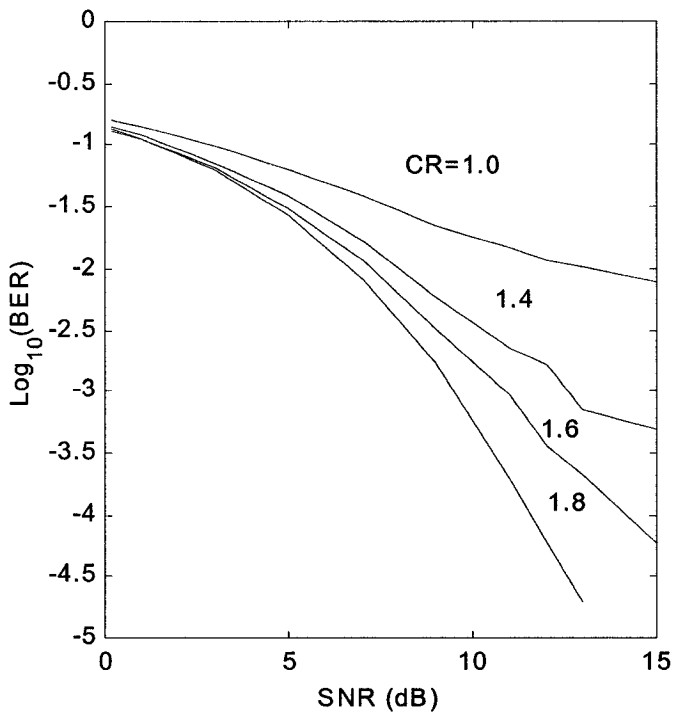

Fig. 3.9 BER given by different clipping ratio

Table 3.2 BER for different CR and SNR values

CR values	BER in SNR=10 (dB)	BER in SNR=12(dB)
CR=1.0	0.045	0.021
CR=1.4	0.0075	0.0035
CR=1.6	0.0035	0.00094
CR=1.8	0.00082	0.000096

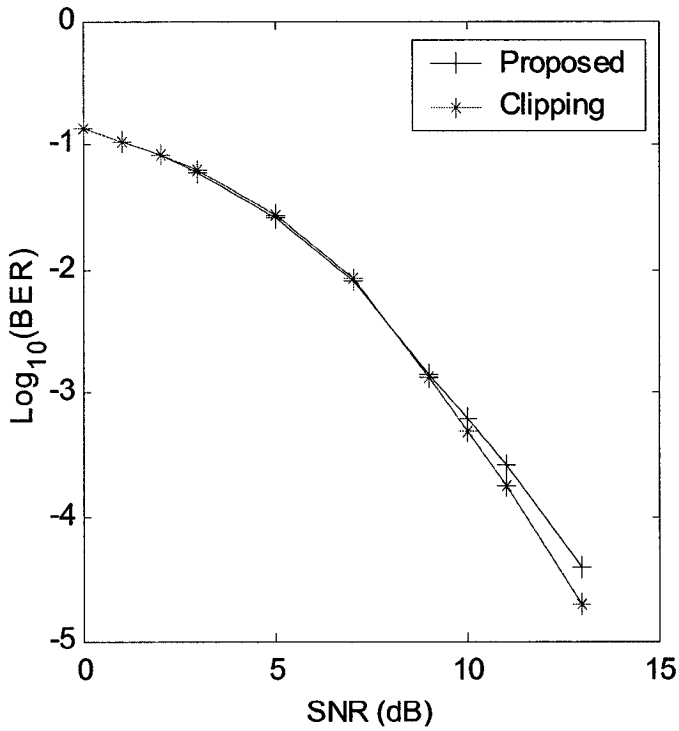

Fig. 3.10 BER performance comparison

Table 3.3 BER for different PAPR reduction techniques

Method	SNR=10 (dB)	SNR=13(dB)
Clipping	0.00075	0.000032
Proposed	0.00078	0.000063

In the above, we have shown the simulation results for the proposed method in terms of the PSD and the BER performance of the OFDM system, resulting from the PAPR reduction. It is seen that the proposed method, in comparison to the conventional clipping method, gives a much better performance with a little sacrifice in the BER

3.3.3 Comparison of the Proposed Scheme with that of Applying the Peak Windowing Alone

In this section, we compare the proposed PAPR reduction method with that of applying the peak windowing alone in terms of the out-of-band radiation and the BER performance. Fig. 3.11 shows the spectrum of the OFDM signal resulting from the application of two methods. It is observed that the signal is about 10 dB higher outside the frequency band if the proposed method is used. With this minor expense, however, one can benefit from a better PAPR reduction as well as the BER performance as seen from Table 3.4 and Fig. 3.12. In this simulation, the clipping ratio is set as 1.8. Fig. 3.12 shows that the proposed method improves the BER performance by about 1.6 dB at 10^{-4} level.

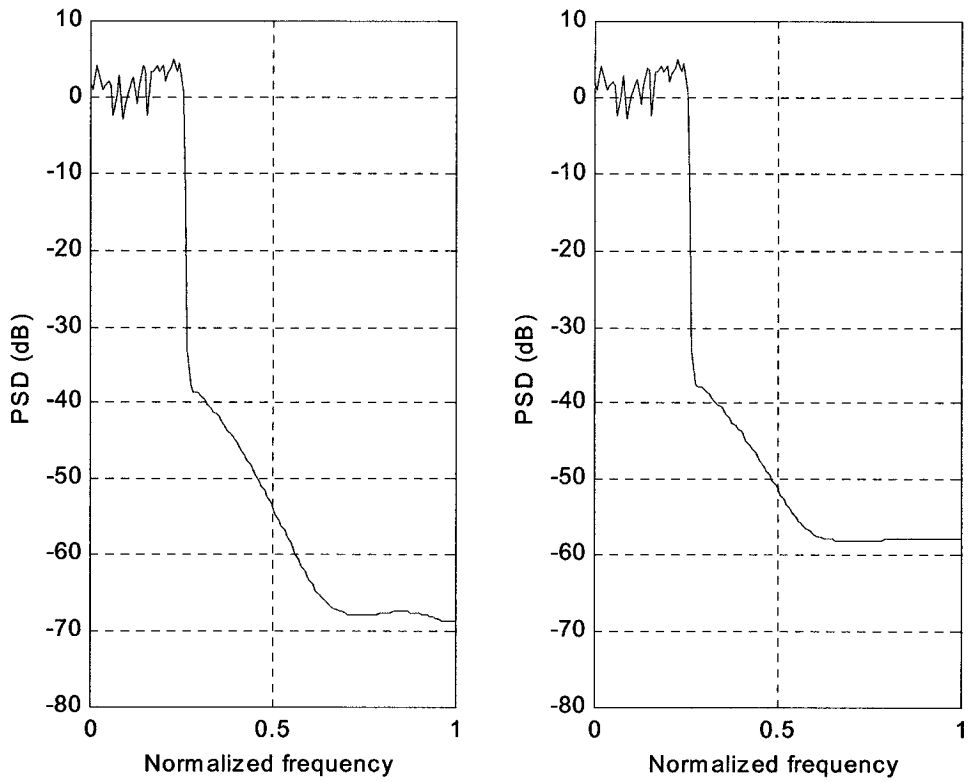

(a) (b)

Fig. 3. 11 PSD of OFDM signal using (a) the peak windowing method, and (b) the proposed approach

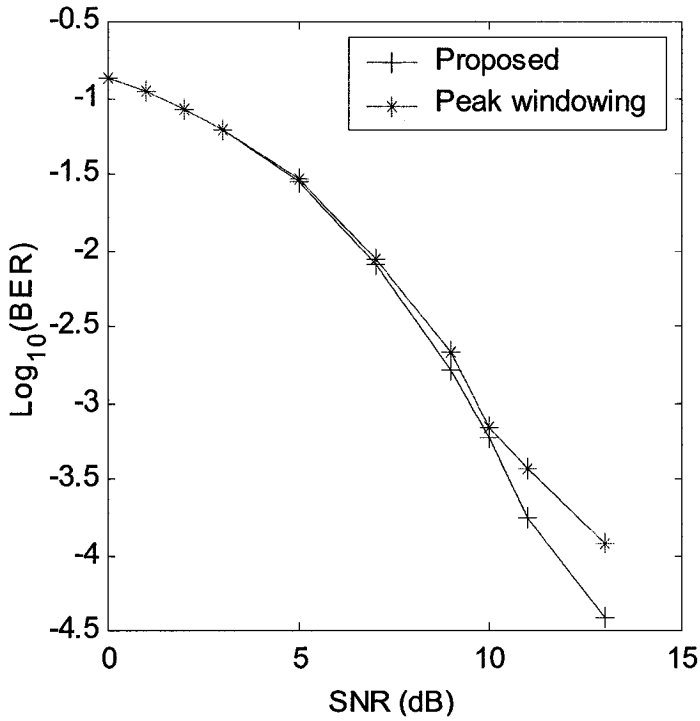

Fig. 3.12 BER performance comparison

Table 3.4 BER values using different PAPR reduction techniques

Method	**SNR=10 (dB)**	**SNR=13 (dB)**
Peak windowing	0.00082	0.00013
Proposed	0.00078	0.000062

3.4 Complexity Analysis

In this section, we compare the computational complexity of the proposed combination scheme with that of the conventional peak windowing and clipping techniques. In the proposed peak windowing plus clipping scheme, a search procedure is first applied to determine the signal peaks. A pre-specified threshold is used throughout the search. Once a peak is found, a window of length L is applied. Assuming that a peak occurs at $i = i_0$, a new search starts at $i = i_0 + L$. In this way, we can avoid the overlapping between the successive windows, and therefore, can save computations in contrast to an exhaustive search. The first round of search continues until the number of the remaining samples in the current OFDM symbol is less than the window length L. Certainly, the first round of search may miss some of the peak samples. Those peaks are recognized in the second round of search and clipped as required by the proposed scheme.

As the computational cost for the IFFT in the OFDM system is common for any signal distortion methods, it is not taken into account for comparison. Assume that M signal peaks are found in the first round of search using the proposed method. Windowing these peak regions require LM multiplications, where L is the length of the window. The peak samples that have been skipped in the first round of search can be found out through the second search step. These peaks are then simply clipped, requiring one multiplication for each clip. If K peak samples are found in the second round of search, the total number of multiplications is given by

$$N_I = LM + K . \tag{3.17}$$

When the conventional peak windowing method is employed, the successive windows might be overlapped, since the search for peak samples is undertaken sample by sample and it is quite possible that the nearest two peaks are apart by less than one window length. As a result, the minimum number of multiplications required by the conventional windowing method is given by

$$N_2 = L(M+K). \tag{3.18}$$

Clearly, the proposed method has achieved considerable computational savings.

It should be mentioned that if a pure clipping scheme is used, the number of multiplications can be reduced to $M+K$, which corresponds to the minimum number of operations. However, the clipped signal would suffer from a serious spectral distortion, and therefore, pure clipping is not recommended for PAPR reduction.

3.5 Conclusion

In this chapter, we have presented a scheme of combining the peak windowing and clipping for PAPR reduction. A modified DFT interpolation scheme has been proposed for the interpolation of the time-domain OFDM signal. A detailed simulation study has been carried out to show the performance of the proposed scheme in terms of the out-of-band signal distortion and the BER performance of the OFDM system. Different choices for window functions, window length and the clipping ratio have been considered in the simulation study, showing their effectiveness in reducing the PAPR. The main results obtained in this chapter can be summarized as follows.

- In comparison to the conventional clipping technique, the proposed scheme is able to decrease significantly the out-of-band radiation of the PAPR-reduced signal at the expense of a slight degradation in the BER performance.
- In comparison to the conventional peak windowing method, the proposed scheme yields a much better BER performance even though it produces a very small out-of-band radiation.
- The influence of the choice of the window functions, the window length and the clipping level ratio on the PAPR reduction performance has been examined. In general, the PAPR reduction performance depends less on the type of the window function chosen than on the window length. The out-of-band radiation gets smaller as the window length increases. However, a large window length degrades the BER performance.
- It has been observed that the choice of the clipping level ratio has a significant impact on the BER performance and PAPR reduction capability of the system. The BER performance can be improved when increasing the value of CR. However, this also increases the PAPR value. Therefore, the clipping level CR should be suitably chosen based on the system requirement.

Chapter 4

PAPR Reduction Using Phase and Amplitude Adjustment Based PTS Approach

4.1 Introduction

In the previous chapter, a new scheme of combining peak windowing with clipping was developed for PAPR reduction. This scheme belongs to the category of signal distortion methods and performs better than the existing signal distortion approaches. In this chapter, we first review a class of non-distortion techniques, namely, the partial transmit sequence (PTS) methods [32]. We then present a new PTS scheme that is based on the adjustment of the phase of each data subblock. With a pre-specified number of iterations, the proposed method gives the best phase vector for a combination of data subblocks in order to provide the smallest PAPR value. We also propose an amplitude adjustment based partial transmit sequence (AAPTS) scheme in order to reduce the implementation complexity for PAPR reduction. The objective is to select a suitable set of scalars for a linear combination of data subblocks that leads to the minimum value of the PAPR.

4.2 Conventional PTS Scheme

It is known that the complex baseband OFDM signal with N subchannels can be represented as

$$x(t) = \sum_{n=0}^{N-1} X_n e^{j2\pi n\Delta ft} \quad 0 \le t \le NT \tag{4.1}$$

where X_n is the complex information symbol transmitted through the subchannel n, $\Delta f = 1/NT$ the frequency spacing, and T the duration of the information symbol. The instantaneous power of $x(t)$ is given by

$$P(t) = |x(t)|^2 = \sum_{n=0}^{N-1}\sum_{m=0}^{N-1} X_n X_m^* e^{j2\pi(n-m)\Delta ft} \quad . \tag{4.2}$$

The PAPR of the transmitted signal can be written as

$$PAPR = \frac{\max|x(t)|^2}{E\left[|x(t)|^2\right]} = \frac{\max\{P(t)\}}{P_{av}} \tag{4.3}$$

where $P_{av} = E[|x(t)|^2]$ represents the average power of the sampled OFDM signal. Theoretically, the upper bound of (4.3) can be as large as N in the QPSK modulation systems [12]. However, the probability of the PAPR to assume this level is extremely small.

In the conventional PTS method, the input data vector, $\mathbf{X} = [X_0,...,X_{N-1}]$, is decomposed into disjoint subblocks or clusters $\mathbf{X}_m$, m=1,2,...,M, each having the same size as **X**, and then these subblocks are linearly combined, namely,

$$\widetilde{\mathbf{X}} = \sum_{m=1}^{M} b_m \mathbf{X}_m \, . \tag{4.4}$$

The objective of PTS method is to determine the M coefficients, b_m (m=1,2, …, M), such that the IDFT of $\widetilde{\mathbf{X}}$, namely,

$$\widetilde{\mathbf{x}} = IDFT\{\widetilde{\mathbf{X}}\} = \sum_{m=1}^{M} b_m IDFT\{\mathbf{X}_m\} = \sum_{m=1}^{M} b_m \mathbf{x}_m \tag{4.5}$$

where $\mathbf{x}_m$ represents the IDFT of $\mathbf{X}_m$, has the minimum PAPR. Since an over-sampled OFDM signal is normally needed for the generation of the continuous-time signal for transmission, the IDFT size in obtaining (4.5) is $N \times L$, where L is the over-sampling rate. The over-sized IDFT of $\widetilde{\mathbf{X}}$ given by (4.4) can be obtained by inserting a certain number of zeros in each $\mathbf{X}_m$. Usually, $b_m's$ in (4.5) are chosen as complex values with unit amplitude, i.e., $b_m = e^{j\phi_m}$, $\phi_m \in [0, 2\pi]$. Thus, (4.5) can be rewritten as

$$\widetilde{\mathbf{x}} = \begin{bmatrix} x_{1,1} & x_{2,1} & \cdots & x_{M,1} \\ x_{1,2} & x_{2,2} & \cdots & x_{M,2} \\ & & \vdots & \\ x_{1,LN} & x_{2,LN} & \cdots & x_{M,LN} \end{bmatrix} \begin{bmatrix} e^{j\phi_1} \\ e^{j\phi_2} \\ \vdots \\ e^{j\phi_M} \end{bmatrix}. \tag{4.6}$$

Therefore, the PTS method is reduced to a problem of searching for the optimum phase vector $\mathbf{F} = [\phi_1, \phi_2, ..., \phi_M]^T$ such that the PAPR is minimized.

In the conventional PTS method, the phase factors are always restricted to a finite set of values, that is,

$$\phi_m \in \left\{ \frac{2\pi l}{W} \middle| l = 0,1,...,W-1 \right\}, \qquad 1 \le m \le M$$

where W is the total number of different values that a phase factor can assume. Fig. 4.1 shows a constellation diagram for the phase factor with W=8.

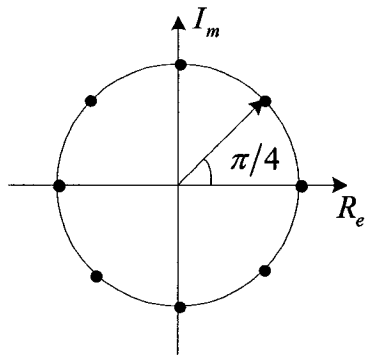

Fig. 4.1 Constellation diagram for the phase factor with W=8

As ϕ_1 can always be fixed without affecting the PAPR, there is a total of W^{M-1} phase searches/iterations. Obviously, an exhaustive search for the optimum phase values is very time-consuming and becomes almost impossible when W is large. Some simplified search schemes have been proposed in the literature. One approach is to limit the phase to a few fixed values such as 0 and $\pi/2$, and then seek an optimum combination. Thus, only 2^{M-1} phase combinations need be tested to find the optimum solution. However, the computational complexity is still quite high when M is large. In the following, we propose a simple phase iteration algorithm to reduce the computational complexity. We will also propose an amplitude adjustment-based iteration algorithm for PAPR reduction.

4.3 Phase Adjustment PTS Scheme

4.3.1 Iterative Algorithm

We now propose a phase adjustment partial transmit sequence (PAPTS) algorithm [46]. The new algorithm searches for the minimum PAPR by employing a pre-specified phase

increment for the update of each phase factor. The phase factor for the mth subblock at the kth iteration can be written as

$$\phi_m^{(k)} = \phi_m^{(0)} + k \cdot \theta_m \tag{4.7}$$

where $\phi_m^{(0)}$ is the initial phase factor and θ_m is the phase increment (stepsize).

Substituting (4.7) into (4.6), we obtain

$$\tilde{\mathbf{x}} = \begin{bmatrix} x_{1,1} & x_{2,1} & \cdots & x_{M,1} \\ x_{1,2} & x_{2,2} & \cdots & x_{M,2} \\ & & \vdots & \\ x_{1,LN} & x_{2,LN} & \cdots & x_{M,LN} \end{bmatrix} \begin{bmatrix} e^{j\phi_1^{(0)}+k\cdot\theta_1} \\ e^{j\phi_2^{(0)}+k\cdot\theta_2} \\ \vdots \\ e^{j\phi_M^{(0)}+k\cdot\theta_M} \end{bmatrix} \tag{4.8}$$

In our study, for the sake of simplicity, $\phi_m^{(0)}$ and θ_m are chosen to be

$$\phi_m^{(0)} = 2\pi(m-1)/M, \qquad (m = 1,2,...,M) \tag{4.9}$$

where M is the total number of subblocks, and

$$\theta_m = \begin{cases} 0, & m = 1 \\ 2\pi/(K-m+2), & m = 2,...,M \end{cases} \tag{4.10}$$

where θ_1 has been set to zero implying that ϕ_1 is fixed as 0, and K is the pre-specified total number of iterations. After k iterations, the OFDM signal can be calculated as

$$\tilde{\mathbf{x}} = \begin{bmatrix} x_{1,1} & x_{1,2} & \cdots & x_{1,M} \\ x_{2,1} & x_{2,2} & \cdots & x_{2,M} \\ \vdots & \vdots & \cdots & \vdots \\ x_{NL,1} & x_{NL,2} & \cdots & x_{NL,M} \end{bmatrix} \begin{bmatrix} 1 \\ e^{j(\frac{2\pi}{M}+k\theta_2)} \\ \vdots \\ e^{j[\frac{2\pi(M-1)}{M}+k\theta_M]} \end{bmatrix}. \tag{4.11}$$

As an example, if the input vector is divided into four subblocks, i.e., $M = 4$, then $\phi_m^{(0)} \in \{0, \pi/2, \pi, 3\pi/2\}$ is used as the initial phase vector. Extensive simulations have shown that the proposed iterative algorithm does not particularly depend on the initial phase vector, that is, different choices of the initial phase factors results only in a slight difference in the PAPR reduction results.

Clearly, the larger the value of K, the more precise search result can be obtained. However, this would require more computations, since PAPR is calculated for each iteration. After the Kth iteration, an OFDM symbol corresponding to the minimum PAPR is found. In order to further reduce the computational complexity, one may specify a threshold for the PAPR. Once the threshold is met, the phase adjustment is terminated. Otherwise, the search continues until K iterations have been carried out.

Fig. 4.2 depicts the implementation diagram of the proposed PAPTS algorithm. The randomly generated binary sequence is first mapped onto QPSK symbols and then partitioned into M subblocks after a serial-to-parallel conversion. An oversized IDFT is used for each subblock. The outputs of the M IDFT blocks are linearly combined using the phase factors. The block Peak value optimizer seeks the best phase vector that minimizes the PAPR of the combined OFDM signal.

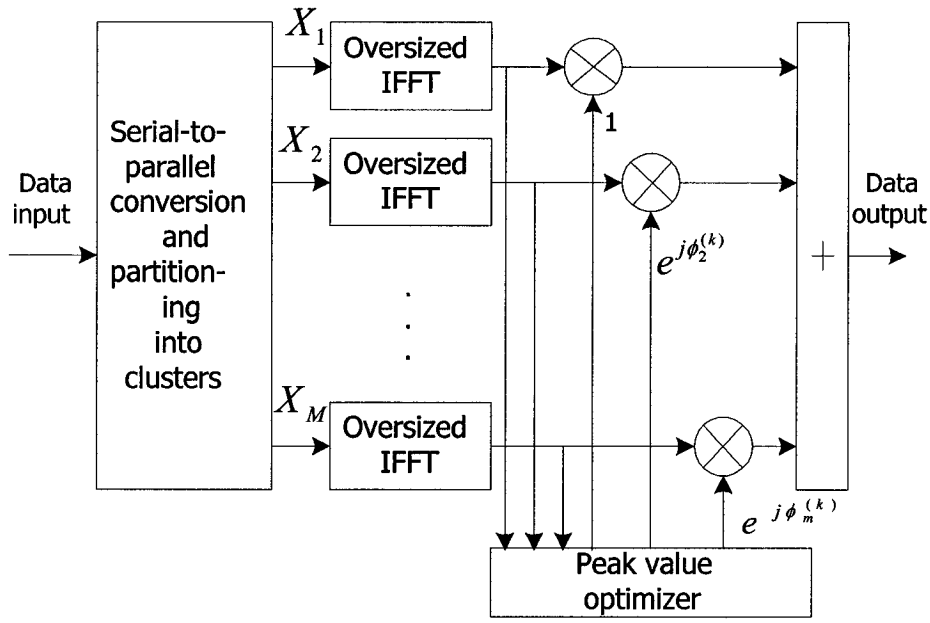

Fig. 4.2 An implementation scheme for the PAPTS algorithm

4.3.2 Simulation Results

To illustrate the performance of the proposed algorithm and compare it with that of the conventional PTS method, in this section, simulation results are presented. The complementary cumulative distribution function (CCDF) of the PAPR employing the proposed scheme is also discussed.

In our simulation, we consider an OFDM system with 256 subcarriers and assume that the OFDM signal is oversampled by a factor of 4, leading to 1024 samples per OFDM symbol, which is sufficient to capture the peak power [39]. The complex input symbols to subcarriers are obtained by QPSK modulation. As a common measure for PAPR reduction performance, the complementary cumulative distributed function (CCDF) of OFDM symbols, which is the probability that the PAPR of the resulting OFDM symbol exceeds a prescribed PAPR threshold $PAPR_0$, is calculated. Moreover, we consider another OFDM system with 128 subchannels in order to illustrate the performance of the

proposed scheme for different number of subcarriers. The parameters chosen for the simulation study are summarized in Table 4.1.

Table 4.1 Parameter configuration for the simulation

Parameter	Configuration
The number of carriers	256, 128
The number of subblocks	2, 4, 8
Rotation phase factors	$\{\pm 1\}$, $\{\pm 1, \pm j\}$
The number of iterations	20, 40, 60, 80, 500

In Fig. 4.3, the complementary cumulative distribution function (CCDF) of PAPR of an original OFDM signal is shown for 256 and 128 subcarriers, respectively, and the corresponding CCDF values are shown in Table 4.2. By comparing these two situations, it is seen that the CCDF performance of PAPR gets worse as the number of carriers increases; however, increasing carriers yields a better spectral efficiency.

(a) Simulation Results for N=256

Fig. 4.4 shows the simulation results obtained from the proposed scheme with 2, 4 and 8 subblocks as well as the result from the conventional PTS method. The CCDF values at the 10^{-2} and 10^{-3} PAPR levels are shown in Table 4.3. It is seen that, By using 8 subblocks, the CCDF performance of the PAPR is improved by 1.2 dB and 2.7 dB, at the 10^{-3} PAPR level compared to the cases of using 4 and 2 subblocks, respectively. Obviously, increasing the number of subblocks would require more IDFT modules, and therefore, increase the computational complexity.

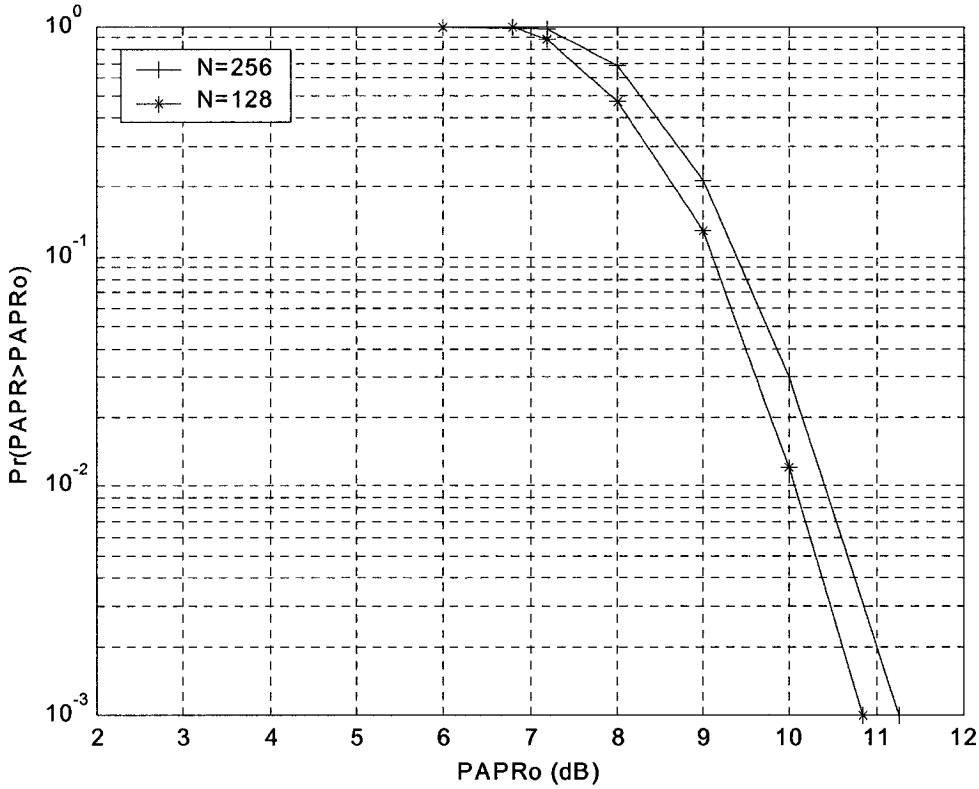

Fig. 4.3 Comparison of CCDF with different number of subcarriers

Table 4.2 CCDF values with different number of subcarriers

Parameters	$PAPR_0$ (10^{-2}PAPR level)	$PAPR_0$ (10^{-3}PAPR level)
N=256	10.40	11.28
N=128	10.05	10.78

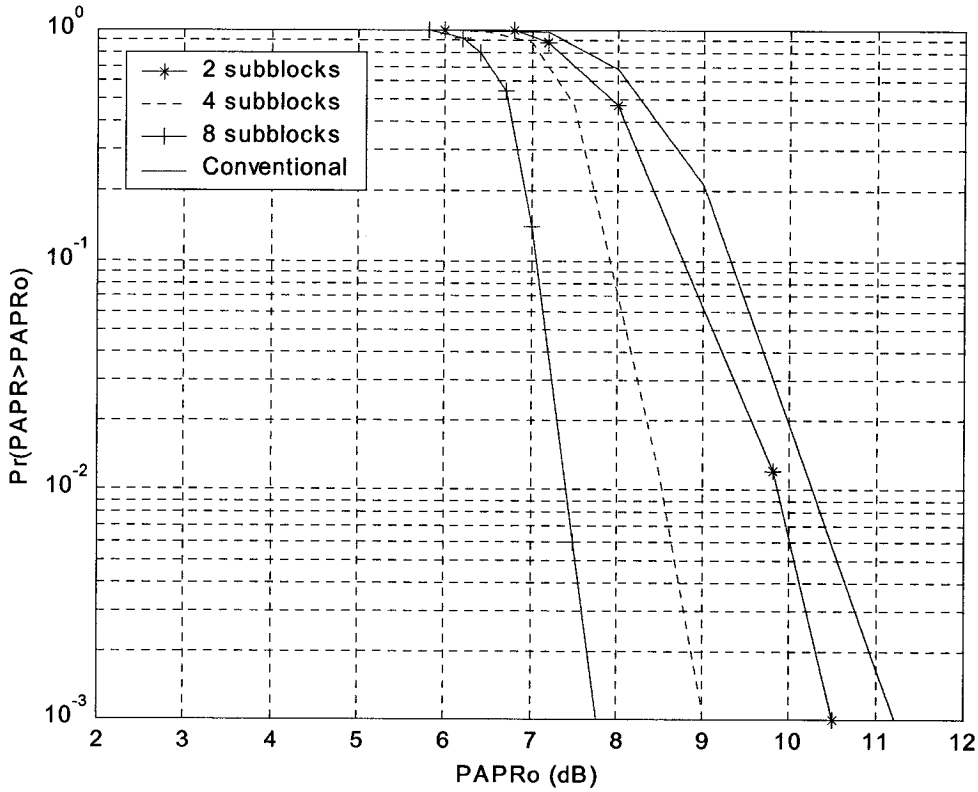

Fig. 4.4 Comparison of CCDF with different number of subblocks

Table 4.3 CCDF values with different number of subblocks

Subblocks (M)	$PAPR_0$ (10^{-2}PAPR level)	$PAPR_0$ (10^{-3}PAPR level)
Proposed M=2	9.88	10.48
Proposed M=4	8.56	9.01
Proposed M=8	7.41	7.78
Conventional	10.40	11.28

In Fig. 4.5, simulation results for a single OFDM block and the case of using 4 subblocks are shown where each subblock is composed of 64 subcarriers. Some of the CCDF values are shown in Table 4.4. It is seen that the original OFDM signal without using PTS has a probability of 0.01 that its PAPR exceeds 10.40 dB. By using the conventional PTS approach with only two phase factors $\{\pm 1\}$ for combination, which requires 8 searches, the PAPR is improved by 1.84 dB at the 10^{-2} level. A similar PAPR reduction performance can be obtained by employing the proposed method with 8 iterations.

Fig. 4.6 shows superior performance of the proposed method when 4 subblocks and 4 phase factors $\{\pm 1, \pm j\}$ are used. Meanwhile, the CCDF values at the 10^{-2} and 10^{-3} PAPR levels are shown in Table 4.5. Note that a total of 64 exhaustive searches is needed by the conventional PTS method, whereas the proposed PAPTS method with 40 iterations gives a very similar CCDF performance. The proposed method results in a performance degradation of less than 0.2 dB at 10^{-2} level. However, the amount of computations is reduced by about 40% by employing the proposed scheme.

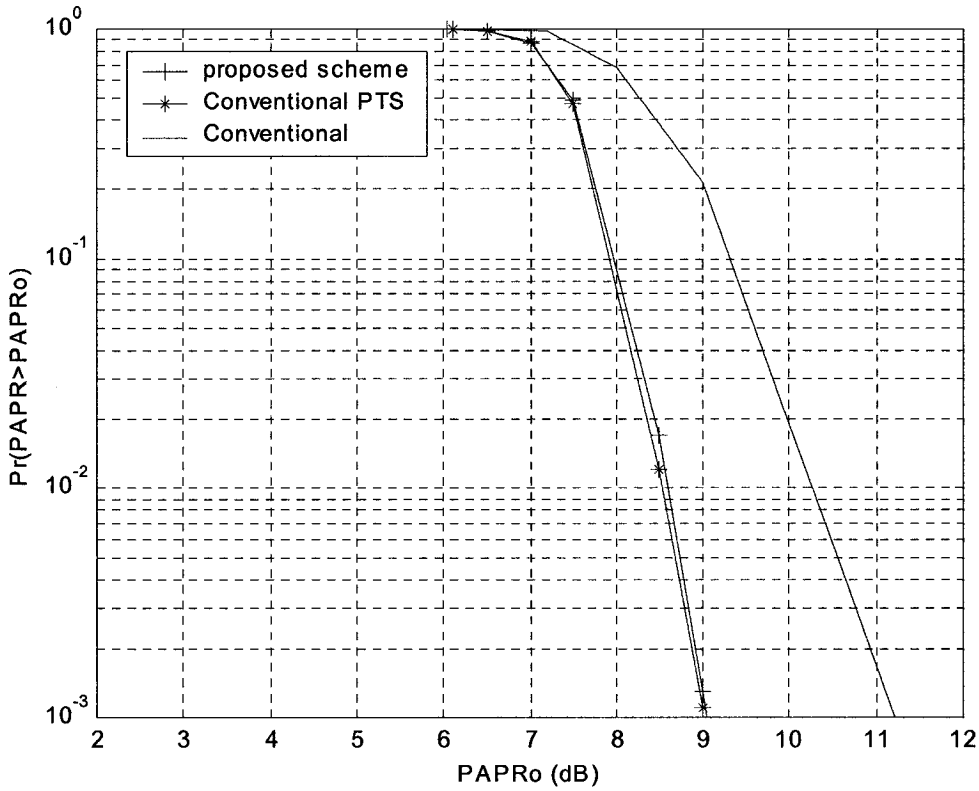

Fig. 4.5 CCDF plot with 4 subblocks and 2 phase factors (N=256)

Table 4.4 CCDF values with 4 subblocks and 2 phase factors (N=256)

Method	$PAPR_0$ (10^{-2}PAPR level)	$PAPR_0$ (10^{-3}PAPR level)
PTS	8.56	9.01
PAPTS (K=8)	8.60	9.03
Conventional	10.40	11.28

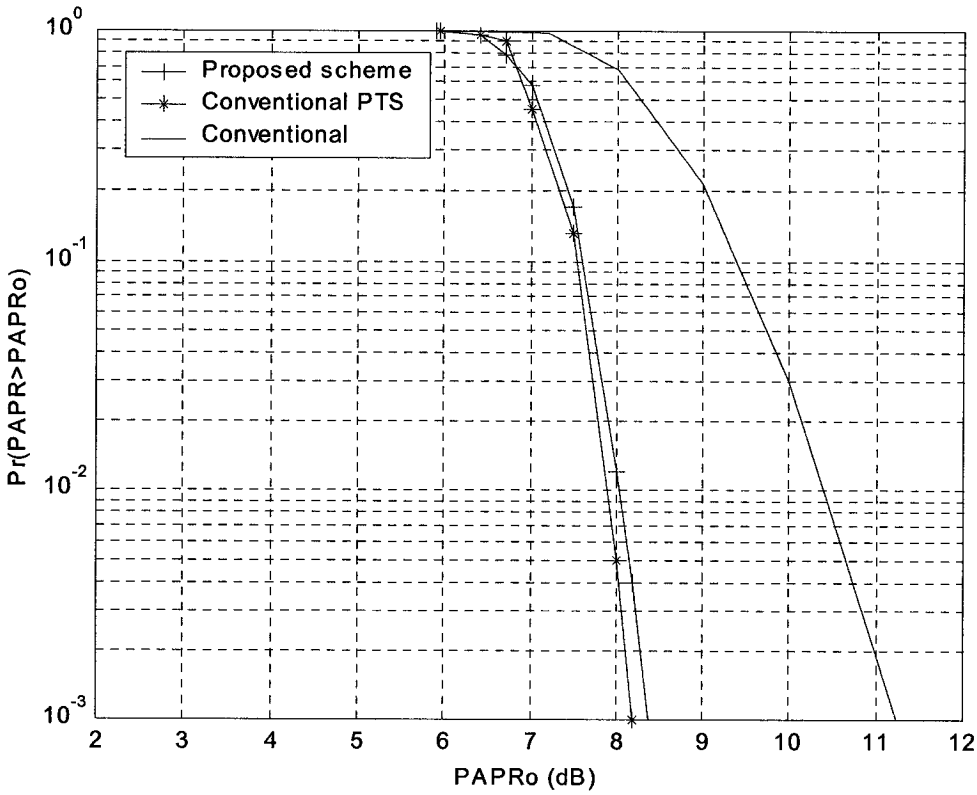

Fig. 4.6 CCDF plot with 4 subblocks and 4 phase factors (N=256)

Table 4.5 CCDF values with 4 subblocks and 4 phase factors (N=256)

Method	$PAPR_0$ (10^{-2}PAPR level)	$PAPR_0$ (10^{-3}PAPR level)
PTS	7.92	8.22
PAPTS (K=40)	8.04	8.40
Conventional	10.40	11.28

Fig. 4.7 shows the result for the case of dividing a single OFDM block into 8 subblocks, where two phase factors {+1, -1} are considered for the conventional PTS scheme. The corresponding CCDF values are shown in Table 4.6. Obviously, 128 searches are needed when using the conventional PTS method. In the PAPTS method, we have chosen K=80. It is seen that by using the PAPTS method, the loss in the PAPR performance is less than 0.2 dB at 10^{-3} probability level while significantly decreasing the computational complexity.

In order to further illustrate the superiority of the proposed scheme, we use 4 different phase factors, $\{\pm 1, \pm j\}$, for an OFDM symbol with 8 subblocks. In this case, the number of exhaustive search of 16384 required by the conventional PTS is very time-consuming. In this simulation, we set K=500 for the PAPTS method. From Fig. 4.8 and Table 4.7, we can see that the CCDF degradation is only 0.17dB at 10^{-3} PAPR level. Thus, the CCDF performance of the proposed scheme is very close to that of the conventional PTS, while providing very significantly computational savings. From the simulation results, we can conclude that the larger the number of subblocks used, the more computational savings can be achieved. In order to further reduce the computational complexity, one may set a threshold to control the number of iterations. Once the threshold is reached, the phase adjustment is terminated. Otherwise, the search continues until the total number of iterations is completed.

Fig. 4.9 shows the simulation results for the PAPTS approach with number of iterations given by K =20, 40 and 60, and the number of subblocks assumed to be M=4. Some of the values from the CCDF plot are also given in Table 4.8. This example shows that the CCDF performance gets better as the number of iterations increases. If the PAPR

of the OFDM system is the main concern, a large value of K is preferred. On the other hand, if the computational complexity is a major concern, a moderate value of K should be used.

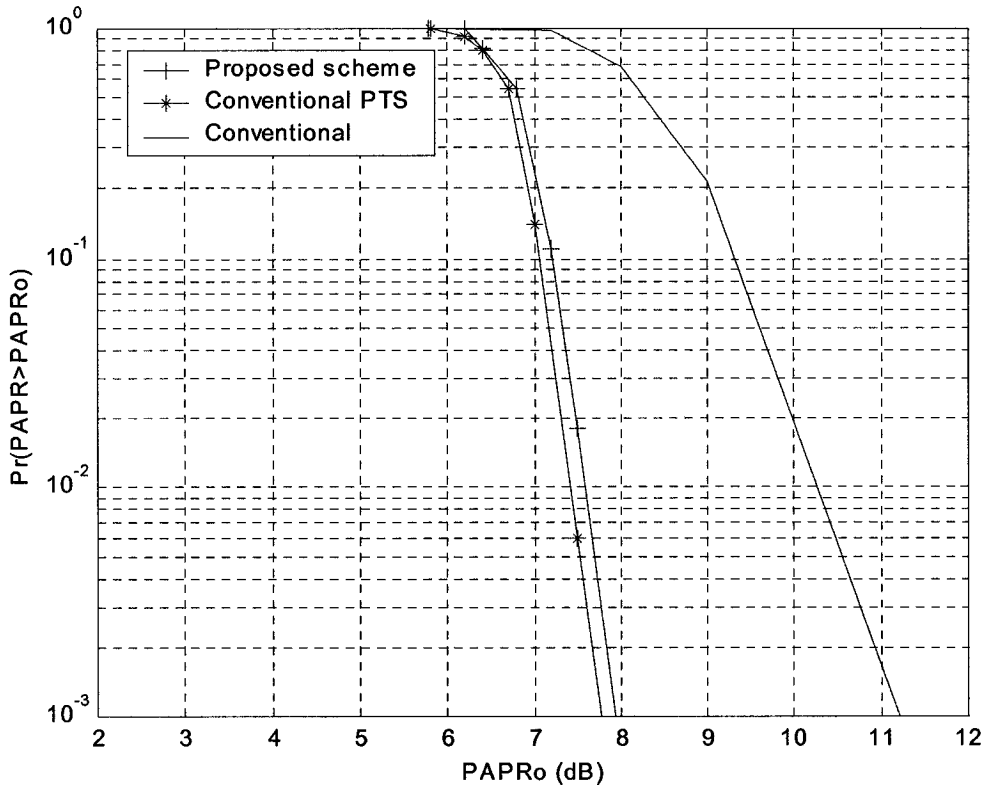

Fig. 4.7 CCDF plot with 8 subblocks and 2 phase factors (N=256)

Table 4.6 CCDF values with 8 subblocks and 2 phase factors (N=256)

Method	$PAPR_0$ (10^{-2}PAPR level)	$PAPR_0$ (10^{-3}PAPR level)
PTS	7.41	7.78
PAPTS (K=80)	7.52	7.96
Original	10.40	11.28

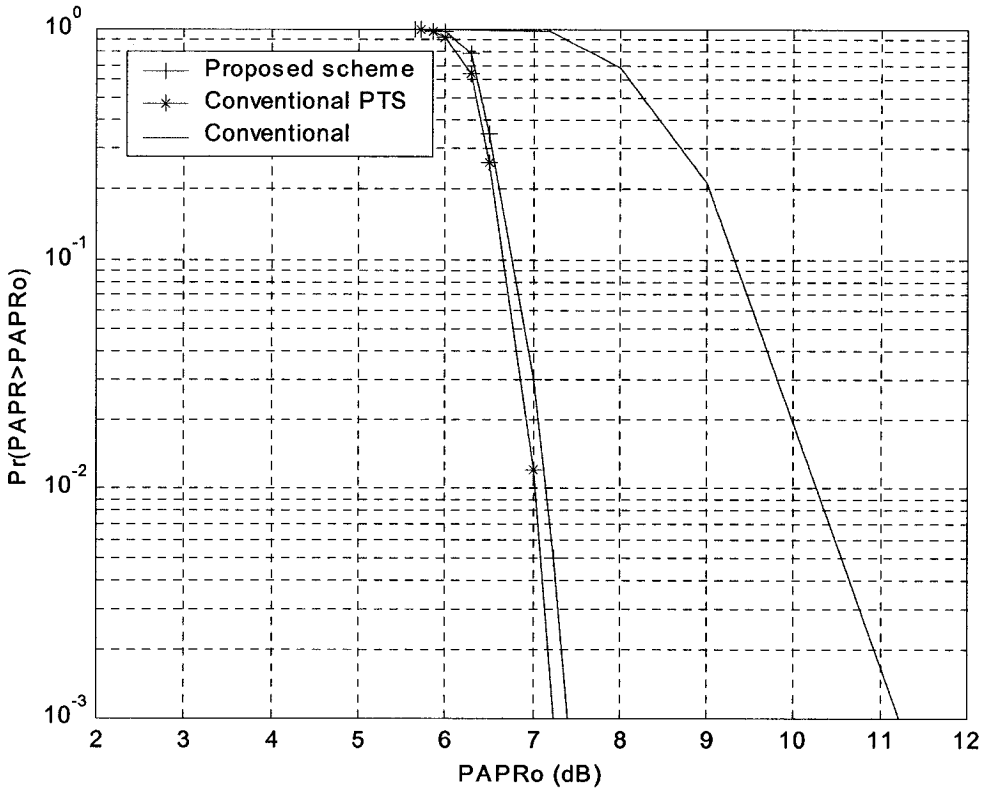

Fig. 4.8 CCDF plot with 8 subblocks and 4 phase factors (N=256)

Table 4.7 CCDF values with 8 subblocks and 4 phase factors (N=256)

Method	$PAPR_0$ (10^{-2}PAPR level)	$PAPR_0$ (10^{-3}PAPR level)
PTS	7.00	7.29
PAPTS (K=500)	7.14	7.46
Conventional	10.40	11.28

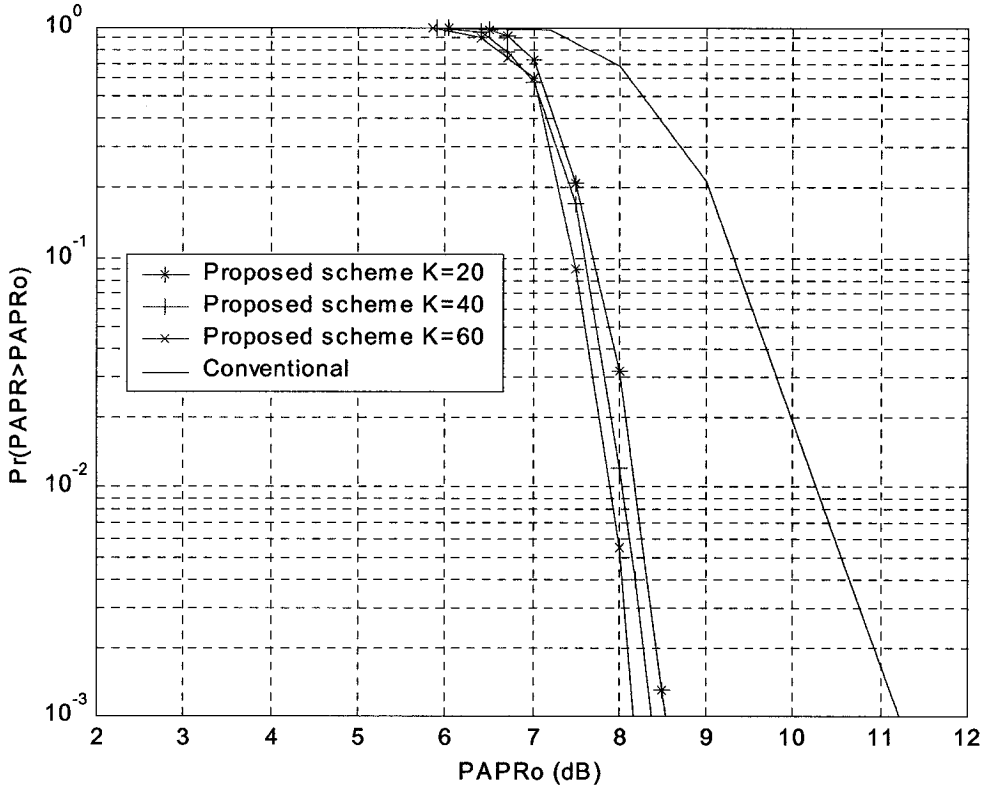

Fig. 4.9 Comparison of CCDF with different number of iterations (N=256)

Table 4.8 CCDF values with different number of iterations (N=256)

Method	$PAPR_0$ (10^{-2}PAPR level)	$PAPR_0$ (10^{-3}PAPR level)
PAPTS (K=20)	8.25	8.58
PAPTS (K=40)	8.04	8.40
PAPTS (K=60)	7.89	8.20
Conventional	10.40	11.28

(b) Simulation Results for N=128

In order to show the performance of the proposed method for yet another number of subcarriers, in this section, we consider 128 subcarriers for the OFDM system. Fig. 4.10 shows the simulation result obtained from the proposed method with 40 iterations in comparison with the result of the conventional method using four phase factors, $\{\pm 1, \pm j\}$. Some of the CCDF values from the plot are also summarized in Table 4.9. The performance degradation of the proposed method in contrast to the conventional PTS is only about 0.04 dB at 10^{-3} probability level, while providing nearly 40% of computational savings.

Next, let us consider the case of segmenting the OFDM signal into 8 subblocks. The same 4 phase factors of $\{\pm 1, \pm j\}$ as in the above simulation are used for conventional PTS scheme. An exhaustive search for the best combination of 8 subblocks requires 16384 searches in calculating the PAPR of the combined OFDM symbol. Nonetheless, the proposed method needs only 500 iterations in order to provide a performance of PAPR reduction similar to that of the conventional method. The CCDF plot and some of the CCDF values from this simulation are shown in Fig. 4.11 and Table 4.10, respectively.

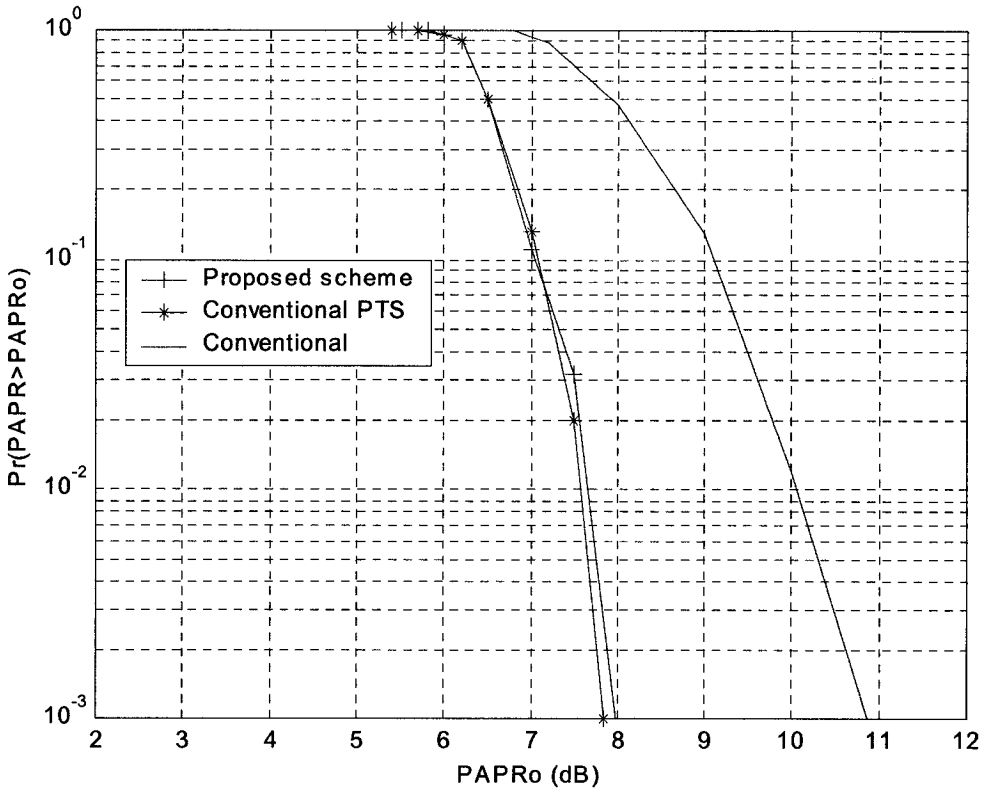

Fig. 4.10 CCDF plot with 4 subblocks and 4 phase factors (N=128)

Table 4.9 CCDF values with 4 subblocks and 4 phase factors (N=128)

Method	$PAPR_0$ (10^{-2}PAPR level)	$PAPR_0$ (10^{-3}PAPR level)
PTS	7.61	7.82
PAPTS (K=40)	7.68	7.98
Conventional	10.05	10.78

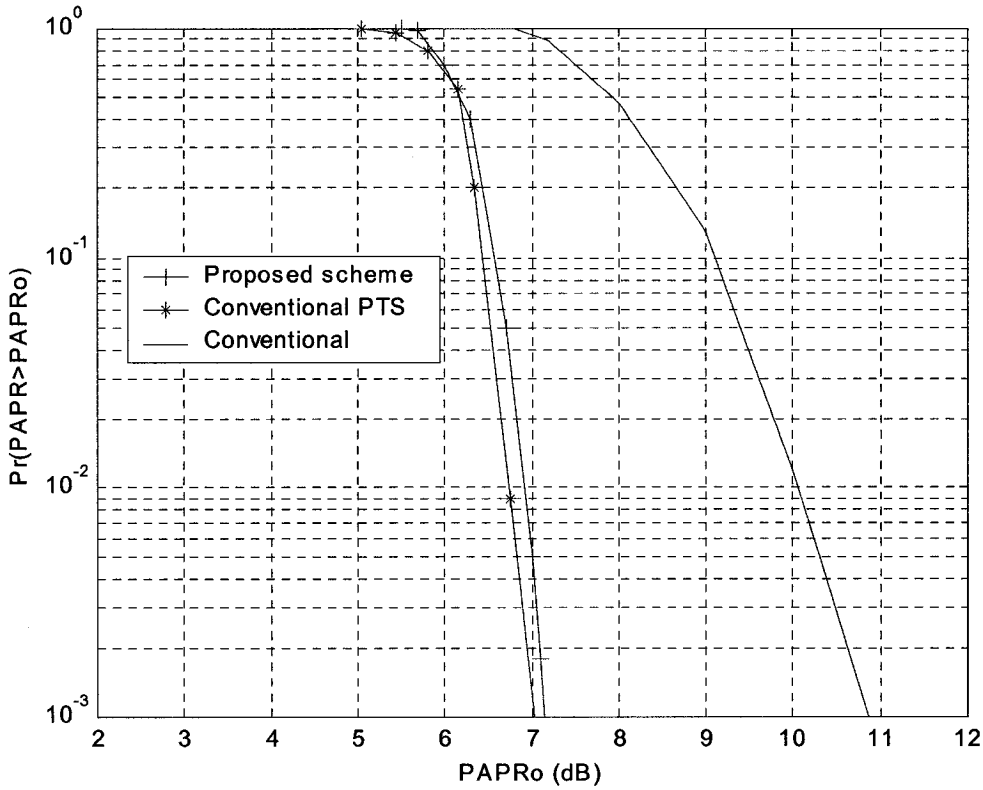

Fig. 4.11 CCDF plot with 8 subblocks and 4 phase factors (N=128)

Table 4.10 CCDF values with 8 subblocks and 4 phase factors (N=128)

Method	$PAPR_0$ (10^{-2}PAPR level)	$PAPR_0$ (10^{-3}PAPR level)
Original	10.05	10.78
PTS	6.76	7.0
PAPTS (K=500)	6.96	7.18

4.4 Amplitude Adjustment PTS Scheme

In this section, a new amplitude adjustment based PTS (AAPTS) algorithm is presented for PAPR reduction. The core of the new algorithm is to seek a set of real scalars for the linear combination of the subblocks so that the PAPR of the combined OFDM symbol is minimized.

4.4.1 The AAPTS Algorithm

Assume that an OFDM symbol is split into M subblocks each undergoing an independent N-point IDFT operation. The linear combination of those subblocks is given by

$$\widetilde{\mathbf{X}} = \sum_{m=1}^{M} r_m \mathbf{X}_m \tag{4.12}$$

where r_m's $(m = 1,2,...,M)$ are the real-valued weighting coefficients. Taking the IDFT of both sides of (4.12) gives

$$\widetilde{\mathbf{x}} = \sum_{m=1}^{M} r_m \mathbf{x}_m \,, \tag{4.13}$$

where $\mathbf{x}_m$ is the IFFT of $\mathbf{X}_m$. The objective is to find a weight vector

$$\mathbf{r} = [r_1, r_2, ..., r_M]^T \tag{4.14}$$

that minimizes the PAPR of $\widetilde{\mathbf{x}}$. Without loss of generality, the first element of $\mathbf{r}$ can be set to unity, i.e., $r_1 = 1$. Thus, the combined OFDM signal can be rewritten as

$$\widetilde{\mathbf{x}} = \begin{bmatrix} x_{1,1} & x_{2,1} & \cdots & x_{M,1} \\ x_{1,2} & x_{2,2} & \cdots & x_{M,2} \\ & & \vdots & \\ x_{1,LN} & x_{2,LN} & \cdots & x_{M,LN} \end{bmatrix} \begin{bmatrix} 1 \\ r_2 \\ \vdots \\ r_M \end{bmatrix}. \tag{4.15}$$

4.4.2 Simulation Results

In this section, the proposed AAPTS algorithm is simulated, CCDF plots for different parameters are obtained. In this simulation, an OFDM system with 256 subcarriers and QPSK-modulated information symbols is considered. The time-domain signal is oversampled by a factor of 4 for transmission. The input data block is partitioned into 4 disjoint subblocks, each represented by vector $\boldsymbol{X}_m$, (m=1,2,3,4). In this study, we propose three sets of weighting vectors, namely, (1) $\{1,1,1,0.2k\}$, (2) $\{1,1,0.1k,0.2k\}$ and (3) $\{1,0.1k,0.2k,0.3k\}$, where k is an integer varying from 1 to K. Clearly, the first set of weight vectors changes the amplitude of one subblock only, the second set allows 2 subblocks to be varied in their amplitude and the third one leaves only one subblock unchanged. Each of the three sets requires a total of K iterations.

Fig. 4.12 shows the simulation results of the proposed AAPTS method using 4 subblocks and the first set of weight vectors $\{1,1,1,0.2k\}$ (k=*1,2, ..., K*), where the number of iterations, K, is set to be 20 and 40. The CCDF performance of the conventional PTS method using 4 phase factors and that of the direct transmission without using PTS are shown in Fig. 4.12 for comparison. Table 4.11 gives some CCDF values from the plot. From Fig. 4.12 and Table 4.11, it is clear that the proposed method provides significant computational savings in comparison to the conventional PTS scheme although the PAPR reduction performance is slightly degraded

Fig. 4.13 depicts the simulation result when using the second set of weight vectors $\{1,1,0.1k,0.2k\}$ (k=*1,2, ..., K*), where K is chosen as 20 and 40. Some of the CCDF values are summarized in Table 4.12 for the purpose of quantitative comparison of the performance of various PAPR reduction schemes for different numbers of iterations.

The amplitude adjustment scheme using the third set of weight vectors $\{1, 0.1k, 0.2k, 0.3k\}$ is also simulated with the CCDF plot shown in Fig. 4.14 and some of its values listed in Table 4.13. The number of iterations is again set to be 20 and 40 for comparison. It is of interest to note that the proposed adjustment scheme using the third set of weight vectors yields a performance that is very similar to that of using first set of weight vectors while it requires more computations. Overall, the proposed adjustment scheme using the second set of weight vectors is superior to that of using first or third set of weight vectors in terms of CCDF performance and computational burden.

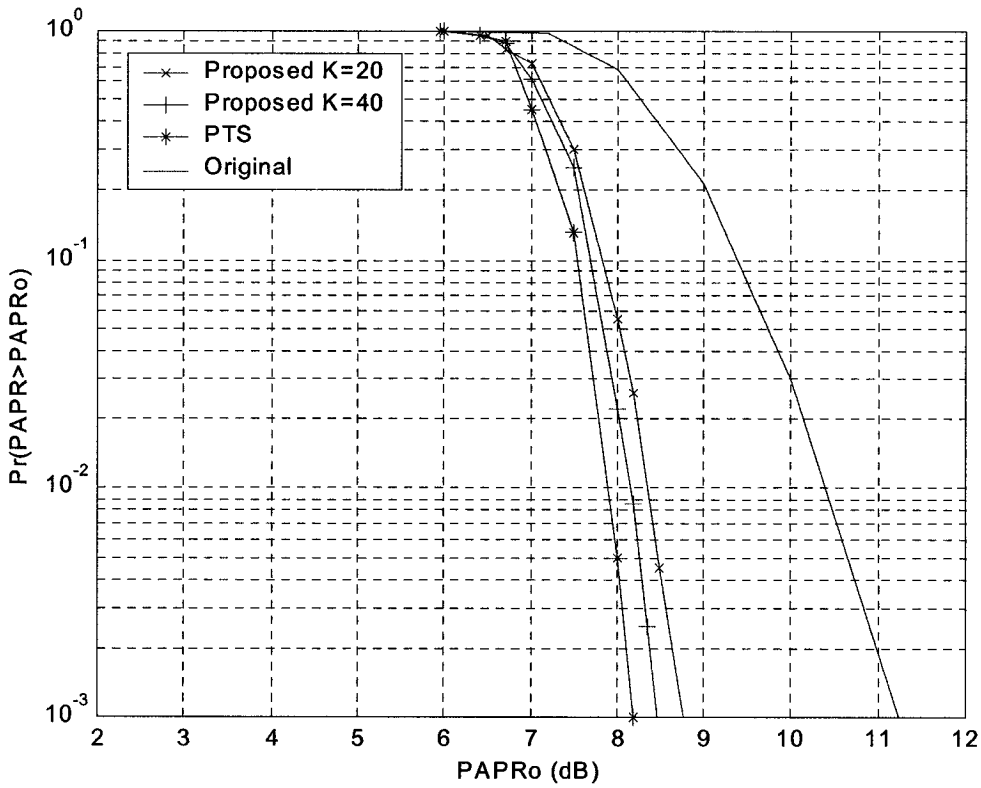

Fig. 4.12 CCDF plot for the case of 4 subblocks with one adjusted subblok

Table 4.11 CCDF values for the case of 4 subblocks with one adjusted subblok

Method	$PAPR_0$ (10^{-2}PAPR level)	$PAPR_0$ (10^{-3}PAPR level)
PTS	7.92	8.22
AAPTS (K=40)	8.15	8.48
AAPTS (K=20)	8.31	8.76
Conventional	10.05	10.78

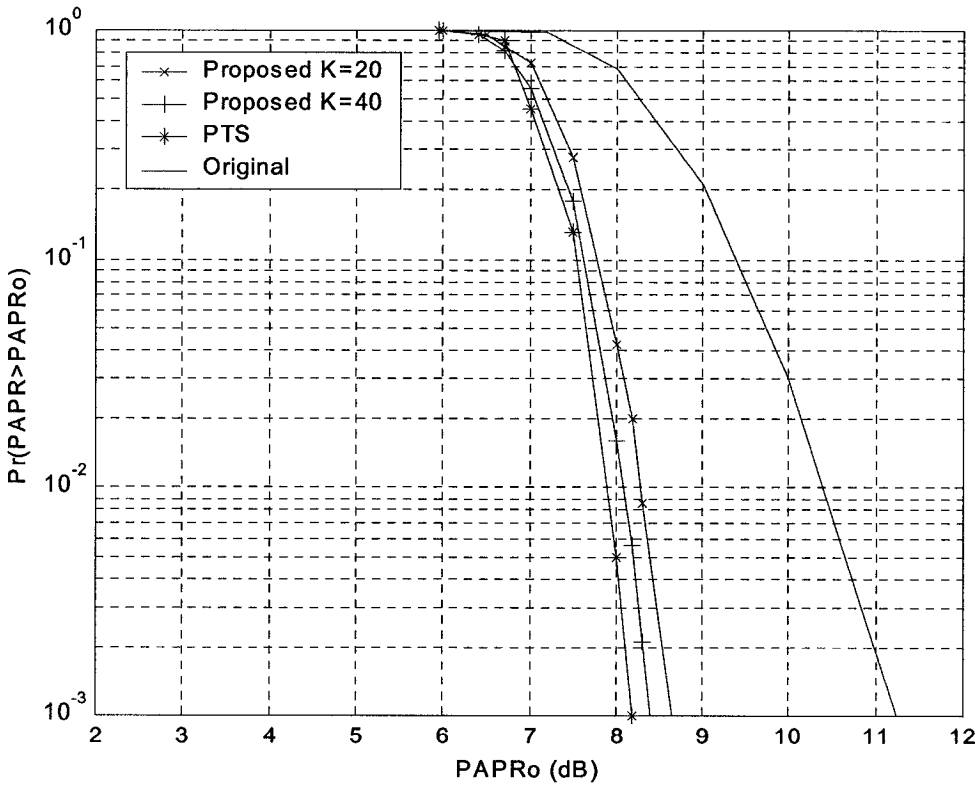

Fig. 4.13 CCDF plot for the case of 4 subblocks with two adjusted subbloks

Table 4.12 CCDF values for the case of 4 subblocks with two adjusted subbloks

Method	$PAPR_0$ (10^{-2}PAPR level)	$PAPR_0$ (10^{-3}PAPR level)
PTS	7.92	8.22
AAPTS (K=40)	8.06	8.45
AAPTS (K=20)	8.25	8.68
Conventional	10.05	10.78

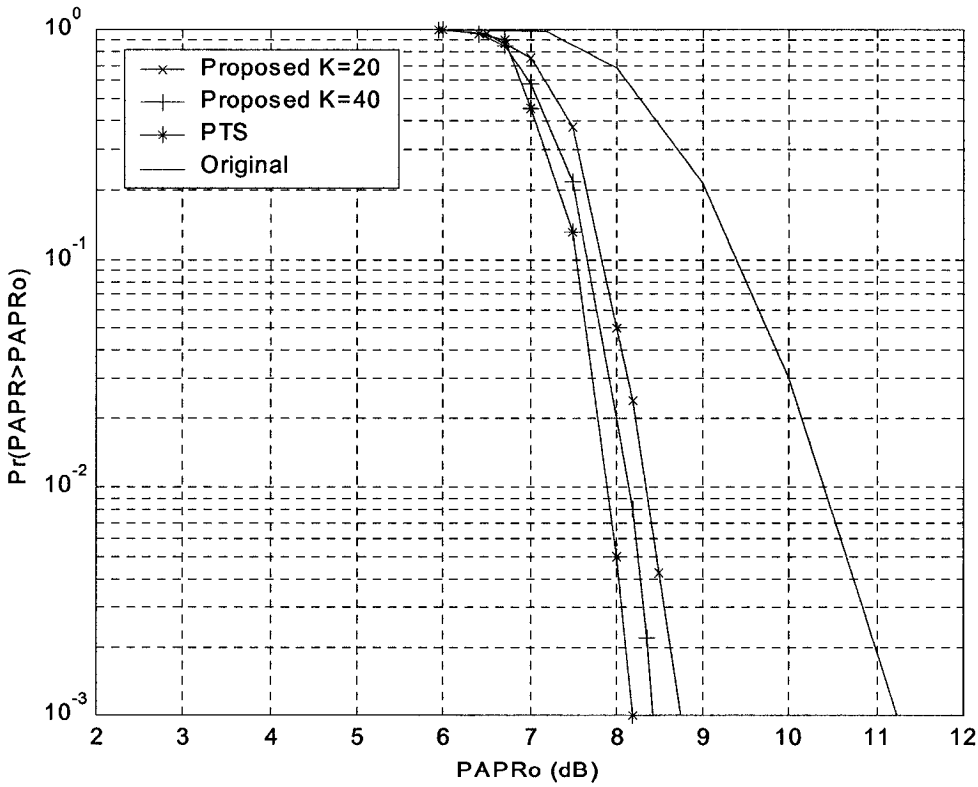

Fig. 4.14 CCDF plot for the case of 4 subblocks with three adjusted subbloks

Table 4.13 CCDF values for the case of 4 subblocks with three adjusted subbloks

Method	$PAPR_0$ (10^{-2}PAPR level)	$PAPR_0$ (10^{-3}PAPR level)
PTS	7.92	8.22
AAPTS (K=40)	8.12	8.48
AAPTS (K=20)	8.28	8.73
Conventional	10.05	10.78

4.5 Conclusion

In this chapter, two new PAPR reduction approaches, namely, the phase adjustment PTS (PAPTS) and the amplitude adjustment PTS (AAPTS), have been presented. In the first approach, the exhaustive search for the best combination of the phase factors that is required by the conventional PTS method has been simplified as an iterative procedure for which the number of iterations can be pre-specified and the amount of computations dramatically decreased. The second approach, which can be viewed as an extension of the phase adjustment PTS method, allows the data subblocks to be adjusted with unequal gains. This second method is more useful in situations where the rotation of each subblock alone may not be able to reduce the PAPR effectively.

The two proposed methods have been simulated to show the impact of various parameters on the PAPR reduction performance. The parameters we have considered in this study include the number of subcarriers, the number of subblocks, the number of iterations, and in the case of the AAPTS method also the weight vectors. The proposed

methods have also been compared with the conventional PTS method in terms of the complementary cumulative distribution function and the computational complexity. Extensive simulations have shown that both the PAPTS and the AAPTS methods are able to yield a PAPR reduction performance that is similar to that of the conventional PTS method and yet to reduce the computational complexity significantly.

Chapter 5

Conclusion and Future Work

5.1 Contributions and Concluding Remarks

In this thesis, a few new PAPR reduction schemes have been presented for OFDM systems. A detailed simulation study has been carried out to show the performance of the proposed techniques and the affects of various parameters employed for PAPR reduction.

In chapter 2, some of the existing signal distortion based PAPR reduction methods, i.e., the peaking windowing and clipping methods, have been reviewed, showing their advantages and disadvantages. In order to overcome the drawbacks of the two signal distortion techniques, a combination scheme of the two techniques has been proposed in chapter 3.

The objective of the proposed scheme is to decrease the PAPR of the OFDM signal while improving the signal spectrum. In the simulation of the proposed scheme, several parameters including the type of window functions, the window length, and clipping ratio (CR) have been considered to evaluate the OFDM system performance. It has been shown that the PAPR reduction performance is less dependent on the type of window functions than the clipping ratio. The PAPR value can be reduced, when a small CR is

used. However, choosing a small value of CR would degrade the BER performance of the OFDM systems.

In chapter 3, the proposed method has also been compared with conventional signal distortion techniques, in terms of the BER performance and the out-of-band radiation. In contrast with the conventional clipping method, the proposed method is able to decrease the out-of-band radiation significantly with a little sacrifice in the BER performance only. On the other hand, the proposed technique yields a better BER characteristic at a small expense of increasing slightly the out-of-band energy in comparison with the conventional peak windowing method.

In chapter 4, two PTS-based PAPR reduction methods using phase and amplitude adjustments, respectively, have been proposed.

The proposed techniques belong to the category of non-signal-distortion method and search for a set of optimum phase or amplitude factors for combining a number of signal subblocks in the optimum fashion that minimizes the PAPR of the overall OFDM signal. In the phase adjustment PTS method, an iterative algorithm has been proposed to seek the optimum phase vector. A thorough simulation study has been conducted to evaluate the PAPR reduction performance of the proposed techniques. Then impact of several parameters, i.e., the number of subblocks, the number of iterations, the phase increment (PAPTS only), etc., on the system performance has also been shown through computer simulation. It has been shown that the proposed PAPTS and AAPTS methods are able to reduce the computational complexity to a certain degree while producing a similar performance in comparison with the conventional PTS method. Furthermore, the PAPR reduction performance can easily be controlled by modifying the parameters employed in

the proposed PAPTS and AAPTS methods. In other words, one can achieve a better PAPR reduction performance easily by allowing the computational complexity to be slightly increased; or one may reduce the computational complexity significantly if a certain degree of performance degradation is tolerable.

5.2 Suggestions for Future Study

The investigation of PAPR reduction for OFDM systems performed in this thesis leads to several thoughts for future study.

- First, the ideal channel characteristic has been assumed in the present simulation study. However, channel fading is a common phenomenon in wireless transmission environments. In order to evaluate the OFDM system performance in real world, multipath fading will be considered in future study. Also, new receiver structure that may incorporate adaptive equalization and channel decoding will be developed.
- Second, most of the existing PAPR reduction techniques are proposed for single user OFDM systems. On the other hand, the elegant properties of OFDM makes it more useful for a wide variety of multi-user applications, such as in the combination of code-division multiple access (CDMA) and OFDM. Therefore, the PAPR issue in multi-user OFDM-CDMA systems will be investigated.
- Third, in multi-user OFDM systems, if the subchannel allocation is not optimized, some of the users may suffer from very serious channel fading. As such, the subchannel allocation for multi-user OFDM systems will definitely be an interesting research topic.

- Lastly, the ideal synchronization has been assumed in the thesis. In a real OFDM system, however, there might exist more or less the inter-carrier interference (ICI), which is caused by the carrier frequency offset. Therefore, the ICI and relevant interference cancellation remedies should be considered in future study of the PAPR reduction issues.

References

[1] Mosier, R.R., and R.G. Clabaugh, "Kineplex, a Bandwidth Efficient Binary Transmission System," *AIEE Trans.* Vol. 76, pp. 723-728, Jan.1958.

[2] "Orthogonal Frequency Division Multiplexing ," *U.S. Patent* No.3,488,4555, filed November 14,1966, issued Jan.6, 1970.

[3] S.B. Weinstein and P.M. Ebert, "Data Transmission by Frequency-Division Multiplexing Using the Discrete Fourier Transform, " *IEEE Trans. Commun. Technol.,* Vol. COM-19, No. 5, pp. 628-634, Oct.1971.

[4] B. Hirosaki, "An Orthogonal-Multiplexed QAM System Using the Discrete Fourier Transform," *IEEE Trans. Commun. Techol.,* Vol. COM-29, No. 7, pp. 982-989, July, 1981.

[5] L.J. Cimini, Jr., "Analysis and Simulation of a Digital Mobile Channel Using Orthogonal Frequency Division Multiplexing," *IEEE Trans. Commun.,* Vol. COM-33, No. 7, pp. 665-675, July 1985.

[6] M. Alard and R. Lassalle, "Principle of Modulation and Channel Coding for Digital Broadcasting for Mobile Receivers," EBU Technical Review, No. 224, pp. 168-190, Aug.1987.

[7] B. Le Floch, R. Halbert-Lassalle and D. Castelain, "Digital Sound Broadcasting for Mobile Receivers," *IEEE Trans. Consumer Electronics.,* Vol. 73, No. 4, pp. 30-34, Aug.1989.

[8] J.S. Chow, J-C. Tu and J.M. Cioffi, "A Discrete Multitone Transceiver System for HDSL Applications," *IEEE J. Select. Areas Commun.*, Vol. 9, pp. 895-908, Aug.1991.

[9] Salzberg, B.R., "Performance of an Efficient Parallel Data Transmission System," *IEEE Trans. Comm.,* Vol. COM-15, pp. 805-813, Dec. 1967.

[10] Porter, G.C., "Error Distribution and Diversity Performance of a Frequency Differential PSK HF Modem," *IEEE Trans. Comm.,* Vol. COM-16, pp. 567-575, Aug. 1968.

[11] H. Sari and I. Jeanclaude, "An Analysis of Orthogonal Frequency Division Multiplexing for Mobile Radio Applications," *Proc. of 1994 IEEE VTC'94,* pp.1635-1639, Stockholm, Sweden, June 1994.

[12] R. van Nee and R. Prasad, "OFDM for Wireless Multimedia Communications", *Boston: Artech House,* 2000.

[13] Wulich, D., Dinur, N. and Glinowiecki, A., "Level Clipped High-Order OFDM," *IEEE Trans. on Commun.,* Vol. 48, No. 6, pp. 928-930, June 2000.

[14] Hideki Ochiai, and Hideki Imai, "On the Distribution of the Peak-to-Average Power Ratio in OFDM Signals", *IEEE Transactions on Communications,* Vol. 49, No. 2, February 2001.

[15] R. van Nee and A. de Wild, "Reduction the Peak-to-Average Power Ratio of OFDM", *IEEE Vehicular Technology Conference,* Vol. 3, pp. 2072-2075, 1998.

[16] X. Li and L.J. Cimini, "Effects of Clipping and Filtering on the Performance of OFDM", *IEEE Communications Letters*, Vol. 2, No. 5, pp.131-133, May 1998.

[17] M. Pauli and H.P. Kuchenbecker, "On the Reduction of the Out-of-Band Radiation of OFDM-Signals" *Proc. of IEEE International Conference 1998,* Vol. 3, pp. 1034-1038.

[18] J. Armstrong, T. Gill and C. Tellambura, "Performance of PCC-OFDM with Overlapping Symbol Period in a Multipath Channel", *IEEE Globecom*, November 2000.

[19] Wulich, D., "Reduction of Peak to Mean Ratio of Multicarrier Modulation Using Cyclic Coding," *Electronic Letters*, 1996, Vol. 32, pp. 432-433.

[20] Davis, J.A., Jedwab, J., "Peak-to-Mean Power Control and Error Correction for Transmission Using Golay Sequence and Reed-Muller Codes," *Electronic Letters*, 1997, Vol. 33, pp. 267-268.

[21] De Wild, A., "The Peak –to-Average Power Ratio of OFDM, " M.Sc. thesis, Delft University of Technology, Delft, The Netherlands, Sept. 1997.

[22] May, T., and H. Rohling, "Reducing the Peak-to-Average Power Ratio in OFDM Radio Transmission Systems," *Proceedings of IEEE VTC'98,* Ottawa, Canada, pp.2774-2778, May 18-21, 1998.

[23] Wilkinson, T.A., and A.E. Jones, "Minimisation of the Peak-to-Mean Envelop Power Ratio of Multicarrier Transmission Schemes by Block Coding," *Proceedings of IEEE Vehicular Technology Conference*, Chicago, pp. 825-829, July 1995.

[24] Golay, M.J.E., "Complementary Series," *IRE Transactions on Information Theory*, Vol. IT-7, pp. 82-87, April 1961.

[25] Sivaswamy, R., "Multiphase Complementary Codes, " *IEEE Transactions on Information Theory*, Vol. IT-24, No. 5, Sept.1978.

[26] Popovic, B.M., "Synthesis of Power Efficient Multitone Signal with Flat Amplitude Spectrum," *IEEE Transactions on Communications*, Vol. 39, No. 7, July 1991.

[27] Van. Nee, R.D.J., "OFDM Codes for Peak-to-Average Power Reduction and Error Correction," *IEEE Global Telecommunications Conference*, London, pp. 740-744, Nov. 18-22,1996.

[28] Van. Nee, R.D.J., "An OFDM Modem for Wireless ATM, " *IEEE Symposium on Communications and Vehicular Technology,* Gent, Belgium, October 7-8,1996.

[29] Davis, J.A., and J. Jedwab, "Peak-to-Mean Power Control and Error Correction for OFDM Transmission Using Golay Sequences and Reed-Muller Codes," *Electronics Letters,* Vol. 33, pp. 267-268, 1997.

[30] Evtvelt, P.V., Wade, G. and Tomlinson, M., "Peak to Average Power Reduction for OFDM Schemes by Selective Scrambling," *Electronics Letters,* Vol. 32, No. 21, pp.1963-1964, Oct. 1996.

[31] Bauml, R., Fischer, R., and Huber, J., "Reducing the Peak-to-Average Power Ratio of Multicarrier Modulation by Selected Mapping," *Electronics Letters,* Vol. 32, No.22, pp. 2056-2057, Oct. 1996.

[32] Muller, S.H., and Huber, J.B., "OFDM with Reduced Peak-to-Average Power Ratio by Optimum Combination of Partial Transmit Sequences," *Electronics Letters*, Vol. 33, No. 5, pp. 368-369, Feb.1997.

[33] Tellambura, C., "Phase Optimisation Criterion for Reducing Peak-to-Average Power Ratio in OFDM," *Electronics Letters,* Vol. 34, No. 2, pp. 169-170, Jan. 1998.

[34] Muller, S., Bauml, R., Fischer, R., and Huber, J., "OFDM with Reduced Peak-to-Average Power Ratio by Multiple Signal Representation", *Annuals of*

Telecommunications, Special issue on *multirate digital signal processing in telecommunication applications,* 1996.

[35] K.P. Prasad and P. Satyanarayana, "Fast Interpolation Algorithm Using the FFT", *Electron, Lett.,* Vol. 22, pp.185-187, 1983.

[36] R.W. Schafer and L.R. Rabiner, "A Digital Signal Processing Approach to Interpolation", *Proceeding of IEEE,* Vol. 61, No. 6, pp. 692-702, Jun. 1973.

[37] J. Armstrong, "New OFDM Peak-to-Average Power Reduction Scheme", *IEEE Vehicular Technology Conference,* pp. 756-760, May 2001.

[38] N. Dinur and D. Wulich, "Peak to Average Power Ratio in Amplitude Clipped High Order OFDM", *Military Communication Conference, 1998, MILCOM 98, Proceedings., IEEE* Vol. 2, 1998.

[39] J. Cimini. Jr., and N.R. Sollenberger, "Peak-to Average Power Ratio Reduction of an OFDM Signal Using Partial Transmit Sequences", *IEEE Communications Letters*, Vol. 4, Issue: 3, pp. 86-88, March 2000.

[40] A.D.S. Jayalath, C. Tellambura and H. Wu, "Reduced Complexity PTS and New Phase Sequences for SLM to Reduce PAP of an OFDM Signal ", *Vehicular Technology Conference Proceedings,* 2000. VTC 2000- Spring Tokyo. 2000 IEEE 51st, Vol. 3, pp.1914-1917, 2000.

[41] C. Tellambura, "Improved Phase Factor Computation for the PAR Reduction of an OFDM Signal Using PTS", *IEEE Communications Letters,* Vol. 5, No. 4, pp.135-137, April 2001.

[42] H. Chen and G.J. Pottie, "An Orthogonal Projection – Based Approach for PAR Reduction in OFDM", *IEEE Communications Letters,* Vol. 6, No. 5, pp.169-171, May 2002.

[43] H. Ryu and K. Youn, "A New PAPR Reduction Scheme: SPW (Subblock Phase Weighting)", *IEEE Transactions on Consumer Electronics,* Vol. 48, No.1, pp. 81-89, February 2002.

[44] S.G. Kang, J.G. Kim, and E.K. Joo, "A Novel Subblock Partition Scheme for Partial Transmit Sequence OFDM," *IEEE Transactions on Broadcasting*, Vol. 45, No. 3, pp. 333-338, Sept. 1999.

[45] A.D.S. Jayalath, and C. Tellambura, "Peak-to-Average Power Ratio Reduction of an OFDM Signal Using Data Permutation with Embedded side Information," *ISCAS 2001*, Vol. 4, pp. 562-565, 2001.

[46] Peng Liu, W.-P. Zhu, and M.O. Ahmad, "A Phase Adjustment Based Partial Transmit Sequence Scheme for PAPR Reduction", accepted for publication in *Circuits, Systems and Signal Processing.*

[47] Proakis, J., "Digital Communications," McGraW Hill, Inc. 1995.